

## Special Section: Hydrological Observatories

### Core Ideas

- A new hydrometeorological observatory was established for the Sudan Savanna.
- More than 30 hydrometeorological variables in subhourly resolution are provided.
- Water, energy, and CO<sub>2</sub> fluxes are monitored along a land use change gradient.
- The data form the basis for an improved impact assessment of environmental changes.
- It is an excellent platform for future field and modeling studies in West Africa.

J. Bliedernicht, L. Hingerl, S. Wagner, A. Straub, R. Schönrock, and H. Kunstmann, Institute of Geography, Univ. of Augsburg, Augsburg, Germany; S. Berger, M. Mauder, R. Steinbrecher, J. Arnault, F. Neidl, C. Jahn, and H. Kunstmann, Institute for Meteorology and Climate Research, Karlsruhe Institute of Technology, Garmisch-Partenkirchen, Germany; S. Salack, S. Guug, A.Y. Bossa, A. Aduna, and B. Barry, Competence Centre, West African Science Service Centre on Climate Change and Adapted Land Use, Ouagadougou, Burkina Faso; D. Heinzeller, Univ. of Colorado Boulder, Cooperative Institute for Research in Environmental Sciences, NOAA/OAR/ESRL/Global Systems Division, Boulder, CO 80305; G. Steup, Y. Yira, and B. Diekkrüger, Institute of Geography, Univ. of Bonn, Bonn, Germany; M. Waongo, Training and Research Dep., AGRHYMET Regional Centre, Niamey, Niger; E. Quansah, Dep. of Physics, Kwame Nkrumah Univ. of Science and Technology, Kumasi, Ghana; A.A. Balogun, Dep. of Meteorology and Climate Science, Federal Univ. of Technology, Akure, Nigeria; S. Wagner, Institute for Industrial Engineering, Fraunhofer IAO, Stuttgart, Germany; C. Klein, Centre for Ecology and Hydrology, Wallingford, UK; U. Gessner and K. Knauer, German Remote Sensing Data Center, German Aerospace Centre, Oberpfaffenhofen, Germany; R. Kunkel, Institute for Bio- and Geosciences, Forschungszentrum Jülich, Jülich, Germany; E.C. Okogbue, Dep. of Meteorology and Climate Science, Federal Univ. of Technology, Akure, Nigeria; A. Rogmann, Center for Development Research, Univ. of Bonn, Bonn, Germany. \*Corresponding author (jan.bliedernicht@geo.uni-augsburg.de).

Received 31 Mar. 2018.  
Accepted 11 Sept. 2018.  
Supplemental material online.

Citation: Bliedernicht, J., S. Berger, S. Salack, S. Guug, L. Hingerl, D. Heinzeller, M. Mauder, R. Steinbrecher, G. Steup, A.Y. Bossa, M. Waongo, E. Quansah, A.A. Balogun, Y. Yira, J. Arnault, S. Wagner, C. Klein, U. Gessner, K. Knauer, A. Straub, R. Schönrock, R. Kunkel, E.C. Okogbue, A. Rogmann, F. Neidl, C. Jahn, B. Diekkrüger, A. Aduna, B. Barry, and H. Kunstmann. 2018. The WASCAL Hydrometeorological Observatory in the Sudan Savanna of Burkina Faso and Ghana. *Vadose Zone J.* 17:180065. doi:10.2136/vzj2018.03.0065

© Soil Science Society of America.  
This is an open access article distributed under the CC BY-NC-ND license (<http://creativecommons.org/licenses/by-nc-nd/4.0/>).

# The WASCAL Hydrometeorological Observatory in the Sudan Savanna of Burkina Faso and Ghana

J. Bliedernicht,\* S. Berger, S. Salack, S. Guug, L. Hingerl, D. Heinzeller, M. Mauder, R. Steinbrecher, G. Steup, A.Y. Bossa, M. Waongo, E. Quansah, A.A. Balogun, Y. Yira, J. Arnault, S. Wagner, C. Klein, U. Gessner, K. Knauer, A. Straub, R. Schönrock, R. Kunkel, E.C. Okogbue, A. Rogmann, F. Neidl, C. Jahn, B. Diekkrüger, A. Aduna, B. Barry, and H. Kunstmann

Watersheds with rich hydrometeorological equipment are still very limited in West Africa but are essential for an improved analysis of environmental changes and their impacts in this region. This study gives an overview of a novel hydrometeorological observatory that was established for two meso-scale watersheds in the Sudan Savanna of Southern Burkina Faso and Northern Ghana as part of the West African Science Service Centre on Climate Change and Adapted Land Use (WASCAL) program. The study area is characterized by severe land cover changes due to a strongly increasing demand of agricultural land. The observatory is designed for long-term measurements of >30 hydrometeorological variables in subhourly resolution and further variables such as CO<sub>2</sub>. This information is complemented by long-term daily measurements from national meteorological and hydrological networks, among several other datasets recently established for this region. A unique component of the observatory is a micrometeorological field experiment using eddy covariance stations implemented at three contrasting sites (near-natural, cropland, and degraded grassland) to assess the impact of land cover changes on water, energy, and CO<sub>2</sub> fluxes. The datasets of the observatory are needed by many modeling and field studies conducted in this region and are made available via the WASCAL database. Moreover, the observatory forms an excellent platform for future investigations and can be used as observational foundation for environmental observatories for an improved assessment of environmental changes and their socioeconomic impacts for the savanna regions of West Africa.

Abbreviations: AMMA, African Monsoon Multidisciplinary Analysis; EC, eddy covariance; GHCN, Global Historical Climatology Network; NIMEX, Nigerian Micrometeorological Experiment; RCM, regional climate model; TERENO, Terrestrial Environmental Observatories; WAM, West African monsoon; WASCAL, West African Science Service Centre on Climate Change and Adapted Land Use; WRF-Hydro, hydrologically enhanced version of the Weather and Research Forecasting Model.

West Africa is a region for which high-quality hydrometeorological measurements are very scarce (Jones et al., 2015). However, such information is needed for a better scientific understanding of hydrological processes and their interactions with the atmosphere and the biosphere. Observational data form the basis for the development of reliable modeling approaches for climate change analyses, as well as for determining the impact of land cover changes in hydrology and other disciplines. Many regions in West Africa are characterized by significant land cover changes due to a widespread conversion of savanna and other ecosystems into agricultural land (Ouedraogo et al., 2009; Knauer et al., 2017), which is expected to continue in the future. Land cover change analysis is the basis for the development of sustainable land management practices that strengthen the resilience of socioecological systems against climate extremes and enhance food security. Moreover, substantial biosphere–precipitation feedbacks have been detected for the West African

savanna (Klein et al., 2017). This was found to be linked to their transitional character between energy and water limitation (Green et al., 2017), rendering them particularly sensitive to land use changes.

To improve our scientific understanding of hydrological processes and their interactions with other environmental processes, advanced observational systems are needed. To tackle this issue, various hydrological observatories with enhanced facilities were established in different regions of the world (Blöschl et al., 2016). Examples are the hydrological observatories (Koch et al., 2016; Qu et al., 2016; Wollschläger et al., 2017) of the Network of Terrestrial Environmental Observatories in Germany (TERENO; Zacharias et al., 2011; Bogena et al., 2012; Kunkel et al., 2013), the Hydrological Observatory and Exploratorium (HOBE) for the Skjern catchment in Denmark (Jensen and Illangasekare, 2011), the Hydrological Open Air Laboratory (HOAL) for the Alps in Austria (Blöschl et al., 2016), and the Cévennes-Vivarais Mediterranean Hydrometeorological Observatory in Southern France (Boudevillain et al., 2011). In contrast with the traditional concept of research catchments in hydrology, hydrological observatories are usually based on long-term equipment to provide information beyond the duration of research projects and with a stronger focus on interdisciplinary research (Blöschl et al., 2016). The data of such observational systems were used by many different studies, for example, for investigating hydrological processes and their interactions (Jensen and Engesgaard, 2011; Ringgaard et al., 2011; Takagi and Lin, 2011; Soltani et al., 2017), for development and comparison of process-based hydrological models (Hingerl et al., 2016; Koch et al., 2016) and compartment-crossing modeling approaches (Butts et al., 2014; Larsen et al., 2014), and for analyses of climate change impacts (van Roosmalen et al., 2011) and hydrological extremes (Delrieu et al., 2005).

Due to the low capacities of many West African institutions, study areas with rich hydrological and meteorological equipment are very limited in West Africa. Densely instrumented study regions were often established for short-term periods (<3 yr) as part of field experiments or campaigns of international research projects such as the Sahelian Energy Balance Experiment (SEBEX; Wallace et al., 1991; Kahan et al., 2006), the Estimation of Precipitation by Satellite- Niger experiment (EPSAT-Niger; Lebel et al., 1992), and the Hydrologic Pilot Experiment in the Sahel (HAPEX-Sahel; Goutorbe et al., 1994; Verhoef et al., 1996; Gash et al., 1997; Lebel et al., 1997), conducted in the late 1980s and in the beginning of the 1990s. More recent examples are the Nigerian Micrometeorological Experiment (NIMEX) for the West African monsoon (WAM) onset period in 2004 (Jegede et al., 2004; Mauder et al., 2007), and the NASA field campaign of the African Monsoon Multidisciplinary Analysis (NAMMA) program during the peak period of the WAM in 2006 (Smith et al., 2012). There are only few cases where hydrometeorological observation networks were operated for >3 yr. Examples are the Dahra test site in Senegal (Tagesson et al., 2015) and the measurement networks of the African Monsoon Multidisciplinary Analysis (AMMA) program

(Lebel et al., 2009; Séguis et al., 2011a), which were established for sites in Central Mali (Mougin et al., 2009), Southwest Niger (Cappelaere et al., 2009), and for the Ouémé River basin in Central Benin (Le Lay et al., 2008; Séguis et al., 2011b). The measurement information provided by these networks was used by numerous observational and modeling studies (Stisen et al., 2008; Guyot et al., 2009; Timouk et al., 2009; Vischel et al., 2009). The AMMA observation network was also intended for long-term operations (Lebel et al., 2009), but a complete operation of such densely instrumented sites and watersheds beyond the lifetime of research projects and programs is usually not possible for the partner institutions in West Africa without any further support.

To improve the availability of high-quality hydrometeorological measurements for West Africa, a network of hydrometeorological observatories was established in the Sudan Savanna belt of Burkina Faso, Ghana, and Benin during the last years (Salack et al., 2018b). The observatories were implemented by a German-African research initiative as part of the West African Science Service Centre on Climate Change and Adapted Land Use (WASCAL, [www.wascal.org](http://www.wascal.org)) program. The novel network consists of three observatories established for several watersheds of the Volta basin (Fig. 1). They range from the Dano watershed in Southwest Burkina Faso to the Sissili and Veia watershed in North Ghana and Central-Southern Burkina Faso to the Dassari watershed in North Benin.

The data of the three WASCAL observatories provide a basis for many field experiments conducted by researchers from various disciplines in this region like cropping experiments (Danso et al., 2018), grazing experiments (Ferner et al., 2015; Guuroh et al., 2018), biological studies (Qasim et al., 2016a,b; Krieg et al., 2017; Stein et al., 2017), land cover change analysis (Knauer et al., 2016) and its impacts (Gessner et al., 2015; Quansah et al., 2015), land degradation and deforestation (Dimobe et al., 2015), and for analyzing uncertainties of near-surface weather observations (Salack et al., 2018b). The data are also needed for many different modeling studies, for example, for the development of coupled atmosphere-hydrology models (Arnault et al., 2014, 2016; Naabil et al., 2017), land surface models (Quansah et al., 2017), and other process-based models in hydrology (Yira et al., 2016).

## Objective and Scientific Questions

The objective of this study is to present a detailed overview of the WASCAL hydrometeorological observatory established for the Sissili and Veia watersheds. The new observatory is based on experiences gained in TERENO (Kiese et al., 2018). It is designed for long-term measuring of >30 hydrometeorological fluxes on the ground and further important environmental variables such as CO<sub>2</sub>, which are rarely monitored in West Africa (Ciais et al., 2011). The high-resolution data of this network are complemented by long-term daily meteorological and hydrological observations from national meteorological and hydrological services, as well as other sources, building the basis for analysis of climate change and land cover change in this region.

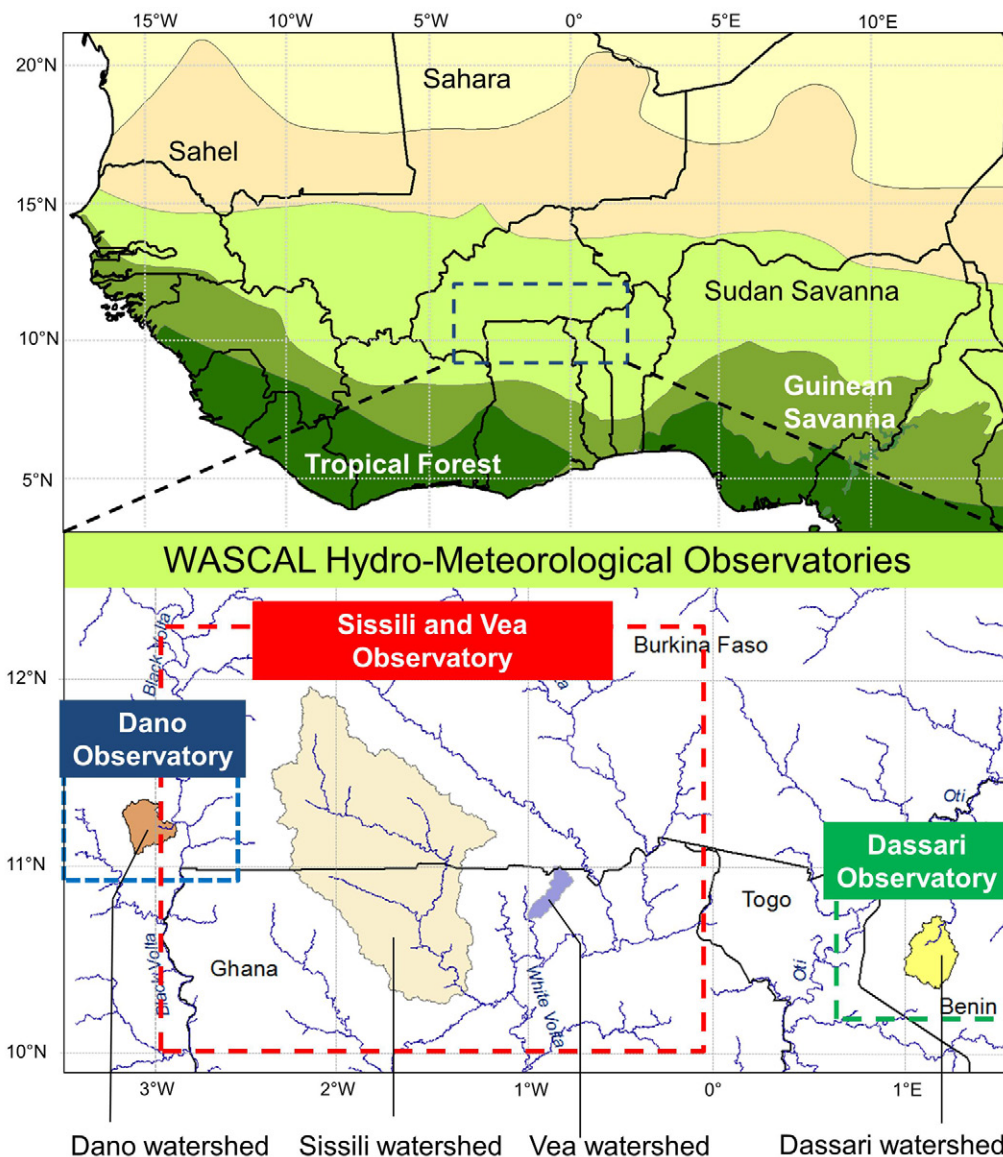


Fig. 1. The West African Science Service Centre on Climate Change and Adapted Land Use (WASCAL) hydrometeorological observatories in the Sudan Savanna belt of Burkina Faso, Ghana and Benin with its focal watersheds (Dano, Sissili, Vea, and Dassari). The watersheds are located in the basins of the main tributaries (Black Volta, White Volta, and Oti) of the Volta River. The upper figure shows the different climatological and ecological zones of West Africa. The map was redrawn from White (1983).

A unique component of this observatory is a micrometeorological field experiment, which was established along a gradient of changing land cover to study the impact of land cover changes on water, energy, and CO<sub>2</sub> fluxes (Bliefernicht et al., 2013; Quansah et al., 2015). The experiment consists of three remotely controlled micrometeorological stations, which are equipped with state-of-the-art eddy covariance (EC) systems (Mauder et al., 2013). Eddy covariance stations are nowadays widely used in many regions of the world and cover various terrestrial ecosystems (Baldocchi et al., 2001; FLUXNET, 2018). However, the number of EC stations is still limited in West Africa, and continuous EC measurements are rarely performed during several years, as shown on the site summary of the FLUXNET data portal (FLUXNET, 2018). The current setup of the EC stations allows onsite estimation of many additional variables, which are usually not measured by standard meteorological equipment, such as heat fluxes and radiation, but also CO<sub>2</sub> fluxes. In this EC experiment, fundamental research questions in the field of land cover change analysis can be addressed for this region:

1. How are climate-relevant land surface properties, such as the albedo, changed by land conversion?
2. What is the impact of land cover changes on the partitioning of water and energy fluxes at the land surface?
3. Can near-natural savanna ecosystems lose their function as a C sink when used for agriculture?
4. How are components of the water balance changed when savanna ecosystems are converted to agricultural land?

An initial description of the new observatory for the Sissili and Vea watershed was presented in Bliefernicht et al. (2013), Quansah et al. (2015), and Salack et al. (2018b). In this study, we aim at giving an updated and more detailed overview of the observatory, including a detailed description of the different networks, the installed devices, and corresponding measured variables. This information is important for a better understanding of the available observation datasets and thus represents an excellent starting basis for future studies using measurements and research findings from this observatory. We will also highlight several technical

challenges (e.g., protection against wildfires) when attempting to establish and operate such an observatory in the West African Sudan Savanna. This provides valuable insights for future establishment and operation of hydrometeorological observatories in West Africa and in many other savanna regions worldwide.

Furthermore, we will present findings of field and simulation experiments conducted for this region using data from the new hydrometeorological observatory. Although a detailed analysis of the 2013 CO<sub>2</sub> fluxes of the observatory was already performed by Quansah et al. (2015), we extend this analysis to the radiation measurements to address the first research question listed above. In addition, an initial evaluation of a novel coupled atmosphere–hydrology model, the hydrologically enhanced version of the Weather and Research Forecasting Model (WRF-Hydro) (Gochis et al., 2013; Senatore et al., 2015; Yucel et al., 2015) is shown, using the micrometeorological measurements of the EC stations. The coupled model was recently applied and evaluated for two watersheds covered by the observatory (Arnault et al., 2016; Naabil et al., 2017) using standard hydrometeorological variables (e.g., precipitation, temperature, and discharge), mainly from global datasets. After these studies, a simulation for a more recent period (2013–2016) was performed, which allowed, for the first time, an evaluation of the coupled simulations for several further hydrometeorological variables (e.g., heat and radiation fluxes) as provided by the WASCAL observatory.

## Description of the Study Region and Catchment Characteristics

### General Description of the Study Area

The study area of the hydrometeorological observatory is located in Southwest Burkina Faso and in Northern Ghana between 10 and 12.5° N and 3 and 0° W. The climate of this region is driven by the WAM (Nicholson, 2013) and can be separated according to the WAM stages into a dry period (December–February), rainy period (July–September), and two transition periods. The annual precipitation amount ranges between 700 and 1100 mm and originates in large parts from mesoscale convective systems. Therefore, precipitation amounts are characterized by a high spatiotemporal variability, in particular for lower spatio-temporal scales, making rainfed farming highly challenging. The study region is also characterized by pronounced multidecadal variability in precipitation, like many other parts of West Africa (Nicholson et al., 2018), which led to several large-scale and long-lasting droughts within the last centuries (Masih et al., 2014), like the severe Sahel drought in the 1970s and 1980s. Although the last two decades exhibited increasing annual precipitation amounts similar to conditions before the 1970s, changing intraseasonal precipitation characteristics (Salack et al., 2016) and an ongoing trend toward more intense convective storms driven by global warming (Taylor et al., 2017) pose new challenges for agricultural applications in West Africa.

The WASCAL hydrometeorological observatory is situated in an area characterized by strong ongoing land cover changes. Like in many other West African countries, the main driver for these changes is the increased food demand of a considerably growing population, mainly resulting from very high birth rates. In Southwestern Burkina Faso, this development was amplified by the migration of people from drought-affected zones in Central and Northern Burkina Faso within the last decades (Ouedraogo et al., 2011, 2009). Consequently, the estimated population growth rate from 1976 to 2007 reached up to 5% yr<sup>-1</sup> in comparison with a country-wide growth rate of ~3% (Ouedraogo et al., 2009; Knauer et al., 2017). Since the income of the majority of people in the Sudan Savanna depends on rainfed agriculture (Ouedraogo et al., 2009, 2011; Forkuor et al., 2017), many regions have been converted to farmland since the 1970s. Several studies showed that the relative increase of farmland can reach up to 1% yr<sup>-1</sup> for Southern Burkina Faso (Ouedraogo et al., 2009, and references therein). The expansion of agricultural land was recently analyzed for Burkina Faso in detail by Knauer et al. (2017).

Due to the severe drought conditions in 1970s and 1980s, many small- to medium-sized water dams were established in the Volta basin (Fowe et al., 2015) to improve the water supply for rainfed farming at community level and to better protect the people from droughts. Liebe et al. (2005) showed that >500 small-sized water dams with a storage capacity between 0.01 and 1 million m<sup>3</sup> are located in the Upper East Region of Ghana. The biggest irrigation dam within the study region is the commercially operated dam of the Tono River basin with a surface area of 18.6 km<sup>2</sup> and a storage capacity of ~93 million m<sup>3</sup> (Dinye and Ayitio, 2013; Naabil et al., 2017). However, high evaporation losses from water dams of up to 60% are a central problem for irrigation practices in this region and can limit their effectiveness (Fowe et al., 2015). Thus, irrigation practices can considerably influence the discharge regime of a river and therefore the water balance of a catchment.

### Sissili River Basin

The Sissili River is one of the main tributaries of the White Volta with a catchment area of ~12,800 km<sup>2</sup> (Arnault et al., 2016). An important advantage of this watershed is the availability of long-term daily discharge measurements, in contrast with many other watersheds in the Volta basin. Long-term daily measurements are usually available for gauges along the main tributaries of the Volta, but tributaries like the Sissili River are often ungauged or have only monthly measurements.

Compared with many other watersheds in the region, land cover changes within the Sissili river basin are less pronounced. This is due to the foundation of a protected wildlife area in the late 1970s, the Nazinga Game Ranch, where no farming activities are allowed. The wildlife area of the ranch is located in the central parts of the Sissili basin, directly at the border between Ghana and Burkina Faso (Fig. 2). It covers an area of ~940 km<sup>2</sup> (Hema et al., 2011), which is 7.2% of the Sissili basin. Since its foundation, many biodiversity studies were conducted in the Nazinga Game Ranch

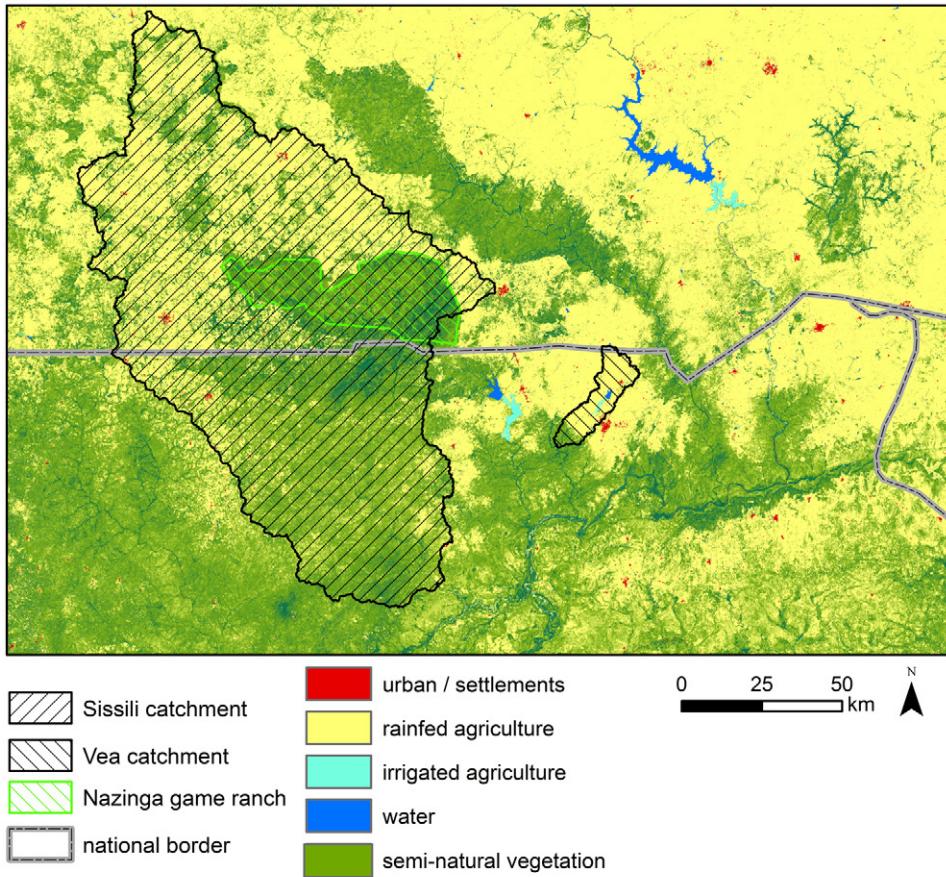


Fig. 2. Land cover and land use patterns in 2014 for the study region. In addition, several important features of the observatory are highlighted: the protected wildlife area of the Nazinga Game Ranch, the basins of the Sissili and Veia Rivers, and two major irrigation dams, the Tono and Veia dam.

(Jachmann, 1991; Jachmann and Croes, 1991; Hema et al., 2011). It is home to one of the few remaining elephant populations in West Africa (Blanc et al., 2007) and various other wildlife species (Marchal et al., 2012). The protected area and its surroundings also served as research and reference site for several other disciplines during the last years, for example, for an analysis of land cover and land use dynamics (Gessner et al., 2015; Knauer et al., 2016; Dimobe et al., 2017) or for performing grazing experiments (Ferner et al., 2015; Guuroh et al., 2018)

Although the Burkinabe parts of the Sissili basin are characterized by a strong population increase within the last decades, many of its areas still have a much lower population density than many other parts of the study region, as shown by Hema et al. (2011) for the surroundings of the Nazinga Game Ranch, or by Barry et al. (2005) for the entire Volta basin. The Sissili basin also has no major reservoirs (like the Tono dam) used for irrigation practices (Barry et al., 2005). We can therefore assume that the discharge regime of the Sissili River is less anthropogenically influenced by rainfed farming and irrigation practices than other watersheds in this region.

### Veia River Basin

The watershed of the Veia River basin is situated in the north-east of Ghana near Bolgatanga. This region is a highly populated area characterized by several spots of strong land degradation (Dietz et al., 2004). The Veia watershed differs from the Sissili basin in many aspects: it is much smaller (~300 km<sup>2</sup>) and is

characterized by a much higher portion of agricultural land. It also contains a major water dam, the Veia dam, which is used for irrigation and water supply of Bolgatanga (Koffi et al., 2017) with an area of 4.5 km<sup>2</sup> and a capacity of 17 million m<sup>3</sup> (Adongo et al., 2014). The relief of the Veia River basin, like the Sissili basin, is relatively flat in many parts of the catchment, with a mean elevation of 196 m and a mean slope of 0.2% (Koffi et al., 2017). Due to the high population density around Bolgatanga, most parts of the Veia catchment are intensively used for agriculture, with several highly degraded spots where cropping activities are no longer possible. An example for these spots is the area around Sumbrungu, where a number of different field experiments were established during the last years (Quansah et al., 2015; Danso et al., 2018).

## Overview of the Observatory

The hydrometeorological network of the observatory is highlighted in Fig. 3 for the study region. This network consists of nine automatic weather stations, one agrometeorological station, three EC stations at four different locations (Supplemental Table S1), and nine hydrological stations. In addition, the precipitation, climate, and hydrological stations of the national weather and hydrological services are illustrated where long-term daily hydrometeorological measurements are available.

The installation of the equipment of the observatory started in September 2012 with the establishment of the EC stations in

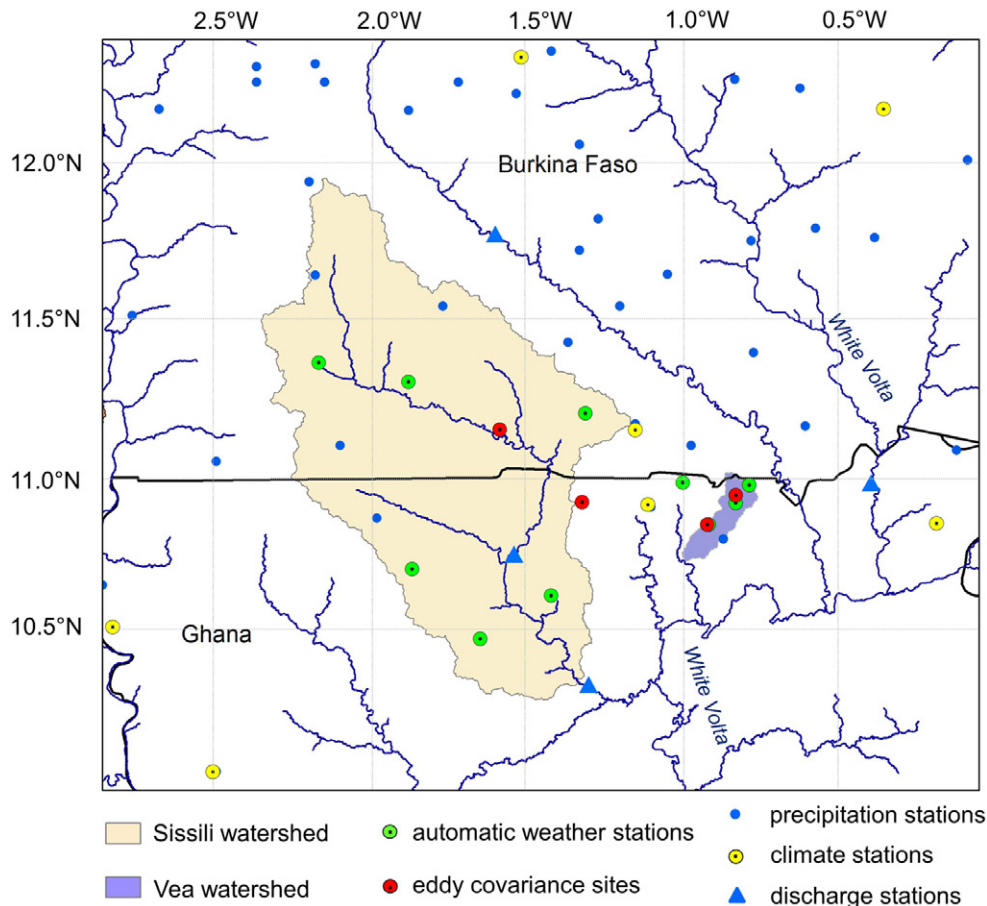


Fig. 3. The different hydrometeorological networks of the observatory for the Sissili and Veá basins. The precipitation, climate, and discharge stations belong to the national and hydrological services of Burkina Faso and Ghana and provide long-term, historical, daily observations. In addition, the automatic weather stations and the four sites of the three eddy covariance (EC) stations are shown. The EC station in Sumbrungu in the lower part of the Veá catchment was relocated due to safety reasons in 2017 to the site Gorigo in the upper part of the basin. The agrometeorological station with its soil water stations is near the EC station in Sumbrungu in the Veá watershed and is therefore not shown in this figure.

Sumbrungu and Kayoro and the automatic weather station in Soe. All further sites were equipped in several subsequent installation campaigns in 2013 and 2014. In 2017, the EC station in Sumbrungu was relocated to Gorigo due to safety reasons (see Technical Challenges section below). Figure 3 also indicates a higher density of the meteorological and hydrological stations around the Veá watershed, providing better data coverage for the different field experiments conducted in this region, in particular at the highly degraded spot in Sumbrungu. In addition to the EC station, the Sumbrungu site also contains an agrometeorological station (Aniabiisi mid-slope) complemented with two further soil water stations (Aniabiisi upslope and downslope), which are installed along a hillslope to support a crop experiment (Danso et al., 2018) with precise hydrometeorological measurements.

## Basic Meteorological and Hydrological Observations

### Subhourly Hydrometeorological Measurements

The automatic weather stations of the network are used to measure seven meteorological variables (Table 1) in 5-min resolution with common meteorological devices. The incoming shortwave radiation is measured by a pyranometer (CS300, Campbell), and a two-dimensional sonic anemometer (Windsonic, Campbell) is used to measure horizontal wind speed and direction.

Air temperature and relative humidity are measured by a silicon bandgap temperature sensor in combination with a capacity humidity sensor (CS215, Campbell), both of which are enclosed in a radiation shield for protection. In addition, a capacity pressure sensor is used to measure air pressure (CS100, Campbell). The total precipitation amount is recorded by a tipping bucket (R. M. Young) mounted to a 1-m-high pole. The other meteorological variables are measured at 2-m height. The power supply for the automatic weather station was established by using solar panels with an additional battery for nighttime measurements. All sensor measurements are collected and stored by a data logger, which is complemented by a data transmission unit to transfer data via Global System for Mobile Communications (GSM) to an external database. A very similar setup is used for the agrometeorological station, but unlike at the automatic weather stations, two further sensors (pyrgeometer and pluviometer) are used for measuring the longwave radiation and precipitation. The soil water station comprises several sensors for determining vertical soil temperature and soil moisture profiles. In addition, tipping buckets are installed at the soil water stations for additional precipitation measurements.

### Long-Term Daily Hydrometeorological Observations

The long-term hydrometeorological observation network of the study region consists of 34 precipitation stations, seven climate

stations, and four discharge stations. Most of the precipitation data were provided by the meteorological services of Burkina Faso and Ghana for a period from 1960 to 2010. The daily precipitation time series are part of a novel database of rain-gauge measurements established for Burkina Faso, Ghana, and Benin. Further data sources of this database are daily precipitation measurements collected from two sources of the Global Change in the Hydrological Cycle (GLOWA) Volta project (Van De Giesen et al., 2002; Laux et al., 2008), the Global Historical Climatology Network (GHCN; Menne et al., 2012), and the AMMA database (Fleury et al., 2011). The daily precipitation measurements of the database are quality controlled following several standards that are similarly used for quality control of the GHCN database (Durre et al., 2010; Menne et al., 2012) and are combined with advanced geostatistical approaches (e.g., spatial correlogram). A subset of this database was recently applied for a performance assessment of a high-resolution regional climate model (RCM; Dieng et al., 2017), for the meteorological analysis of a heavy rainfall event that caused major flooding in Ouagadougou in September 2009 (Engel et al., 2017), and for rating and scaling historical heavy rain events in the region (Salack et al., 2018a,b).

Besides the precipitation database, we also started to establish a database for several meteorological variables with daily measurements from 1980 to 2010. This database consists of temperature variables (minimum daily temperature [ $T_{\min}$ ], maximum daily temperature [ $T_{\max}$ ], and mean daily temperature [ $T_{\text{mean}}$ ]), mean sea-level pressure, horizontal wind speed, and wind direction, as well as humidity variables. The meteorological data are based on daily measurements from the Volta Basin Authority Geoport, which hosts data collected and generated by the GLOWA Volta project, complemented by daily measurements from the GHCN network and the Global Surface Summary of the Day (GSOD) database. Long-term hydrological measurements are only available for the Sissili River basin for two gauges located at the catchment

outlet and further upstream. The data are available from 1960 to 2009 but contain ~40% of missing values. The data were obtained from the Volta Basin Authority Geoport and then combined with more recent measurements from hydrological services in Ghana.

## Hydrometeorological Characteristics of the Study Area

Some meteorological characteristics of the study area, using the information from the hydrometeorological observatory, are shown for the experimental site in Sumbrungu in Fig. 4. The dry period lasts from the beginning of December until the end of February and is characterized by very low precipitation probabilities ( $p_0 < 2\%$ ), hot daytime temperatures ( $33.5^\circ\text{C} < T_{\max} < 38.0^\circ\text{C}$ ), and relatively cool nighttime temperatures ( $T_{\min} < 20^\circ\text{C}$ ), mainly in December and January. During the dry period, northeasterly Harmattan winds prevail, as indicated by the wind roses for January 2013. This regional wind system transports dry air masses from the Sahara to the West African Sudan Savanna. The hottest period in the study region occurs at the end of March ( $T_{\max} = 39.0^\circ\text{C}$  and  $T_{\min} = 26.4^\circ\text{C}$ ), immediately before the onset of the WAM. This period is also characterized by changing wind conditions toward southwesterly monsoonal winds and strongly increasing precipitation probabilities linked to the northward propagation of the intertropical convergence zone. Accordingly, the period when the monsoon reaches its northernmost extent, southwesterly winds are dominant, as illustrated for June 2013 in Fig. 4. These southwesterly monsoon winds transport wet air masses from the Atlantic Ocean to the study area, leading to very humid conditions with much lower diurnal temperature variability. This period is also characterized by the highest rainfall probabilities ( $p_0 > 30\%$ ), reaching up to 50% at this site. The monsoon peak, in terms of daily precipitation amounts, is reached at the end of August with a maximum value of slightly above  $9 \text{ mm d}^{-1}$ . During the cessation period, the monsoon weakens quickly, leading to much drier conditions due to the equatorward retreat

Table 1. Basic measurement characteristics for each variable of the automatic weather stations.

ID	Variable	Type	Characteristic†							
			H	TR	Min.	Max.	R	U	rU	
			m	min						%
1	Incoming shortwave radiation, $\text{W m}^{-2}$	Mean	2	5	0	2000	1	‡		5
2	Air temperature, $^\circ\text{C}$	Mean	2	5	-40	70	0.01		0.3	‡
3	Relative humidity, %	Instantaneous	2	5	0	100	0.05		‡	2
4	Horizontal wind speed, $\text{m s}^{-1}$	Mean	2	5	0	60	0.01		‡	2
5	Horizontal wind direction, $^\circ$	Mean	2	5	0	359	1		3	‡
6	Precipitation, mm	Sum	1	5	0	‡		0.1		‡
7	Air pressure, hPa	Mean	2	5	600	1100	0.01		0.3	‡

† H, measurement height; TR, temporal resolution [min], Min., minimum measurement value; Max., maximum measurement value; R, resolution of the measurement value; U, minimum absolute measurement uncertainty; rU, minimum relative measurement uncertainty; the information on Min., Max., R, U, and rU is based on the user manuals of the corresponding measurement devices. The unit of the measurement characteristics (min., max., R, and U) are variable dependent and are listed in the Variable column.

‡ No information is given.

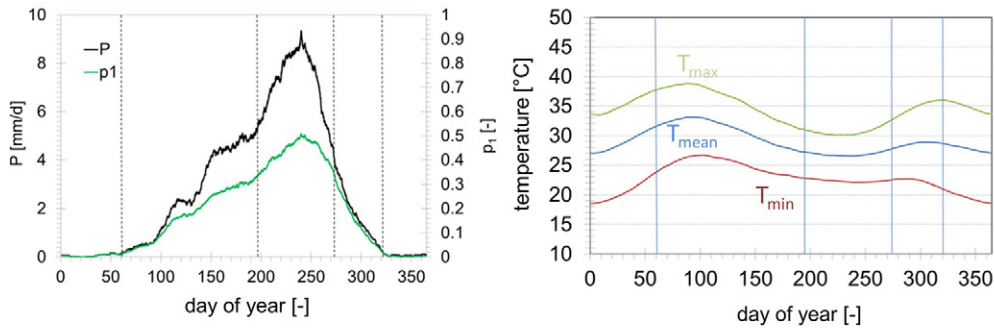


Fig. 4. Basic meteorological characteristics of the study region illustrated exemplarily for the experimental site in Sumbrungu near Bolgatanga in Northern Ghana. The seasonal cycles (upper diagrams) of the daily precipitation amount ( $P$ ), precipitation probability ( $p_1$ ), and daily mean, minimum, and maximum temperatures ( $T_{\text{mean}}$ ,  $T_{\text{min}}$ , and  $T_{\text{max}}$ ) are based on long-term daily precipitation (1960–2010) and temperature measurements (1980–2010). The daily time series were reconstructed from the five closest meteorological and precipitation stations. The wind patterns (lower diagrams) are from sub-hourly observations made at the eddy covariance station in Sumbrungu in 2013.

of the intertropical convergence zone. During this time, the region experiences a second temperature maximum and increasing diurnal temperature variations due to much drier atmospheric conditions.

The database of long-term daily precipitation measurements was also used to generate high-resolution gridded precipitation datasets for different temporal scales (daily, monthly, and annual) using ordinary kriging. The mean precipitation amount of the annual product is shown for the study area in Fig. 5. It shows a distinct north–south precipitation gradient for the study region with ranges from ~700 mm in the northeastern parts to 1100 mm in the southeastern parts of the study region. Moreover, the annual precipitation amounts can vary considerably from year to year, as shown for two EC sites (Sumbrungu and Nazinga) of the observation network in Fig. 6. The diagram also highlights the strong decadal variability of the annual precipitation at both sites with much drier conditions from the mid-1970s to the mid-1980s.

The discharge regime of Sissili River is illustrated in Fig. 7. During the onset period, the runoff generation is much lower in comparison to the peak and cessation period of the WAM. This indicates that most of the rainfall evaporates or refills the groundwater and soil water storages. The maximum daily discharges are reached at the end of August and show a lag of several days with respect to the peak value of the daily precipitation amounts due to hydrological retention and translation processes within the catchment.

## ♦ Micrometeorological Field Experiment

### Description of the Eddy Covariance Sites

The long-term micrometeorological field experiment was performed at four different sites with the three EC stations described

above. The measurement sites are characterized by different vegetation covers due to different land use practices (degraded grassland used for grazing, cropland grazed by livestock, and near-natural vegetation due to wildlife conservation). Other site characteristics such as climate, soil, or topography chosen were as similar as possible to ensure that any long-term difference between the analyzed variables were mainly the result of land cover changes and not of other sources. A detailed overview of the sites characteristics is shown in Table 2. The site selection was done in April 2012 for Sumbrungu and Nazinga, in October 2012 for Kayoro, and in March 2017 for the new site, Gorigo.

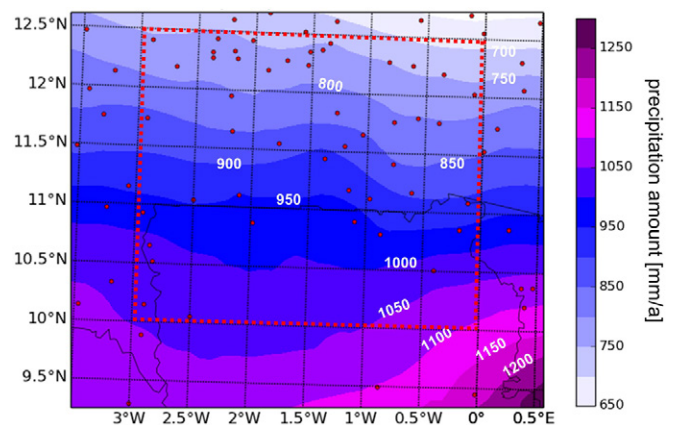


Fig. 5. Spatial distribution of the annual precipitation amounts for the study region. The area of the observatory for the Sissili and Veawatersheds is indicated by the red frame. The annual precipitation amounts are based on long-term daily measurements from 1960 to 2010 using a novel precipitation database of rain-gauge measurements established for Burkina Faso, Ghana, and Benin. The red dots indicate the locations of the precipitation gauges used for spatial interpolation.

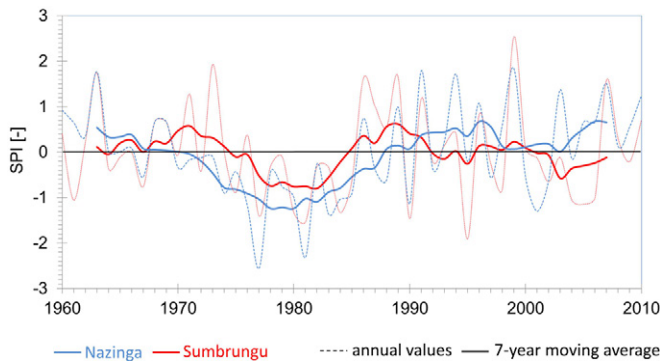


Fig. 6. The decadal variability of the annual precipitation amounts for the eddy covariance station in Nazinga (arithmetic mean = 978 mm yr<sup>-1</sup>, SD = 152 mm yr<sup>-1</sup>) and in Sumbrungu (arithmetic mean = 960 mm yr<sup>-1</sup>, SD = 179 mm yr<sup>-1</sup>); The standard precipitation index (SPI) shown in this diagram is based on a normal-score-transformation using annual precipitation amounts. Positive values indicate wetter-than-average years, negative values indicate drier-than-average years. The annual precipitation amounts for both experimental sites are based on daily precipitation time series reconstructed from the five nearest stations of the surrounding precipitation network.

The EC station for the strongly degraded grassland site was located in Sumbrungu from October 2012 until November 2016. The surrounding area of this EC station (<200 m) is mainly used as rangeland for livestock. Due to the grazing activities and the degraded soils, the mean grass height is usually not >10 cm, even in the rainy season. Supplemental Fig. S1 shows that the EC station is surrounded by a sparse network of medium-sized trees (<6 m) and shrubs. Due to thievery and vandalism, the EC station was relocated to another grassland site with similar characteristics in May 2017 to continue the experiment. This site is located in the upper part of the Vea watershed in a less populated area. A picture of the new EC station Gorigo is shown in Supplemental Fig. S2. The near-natural site is located in a dedicated area for research studies within the core protection zone of the Nazinga Game Ranch wildlife area. The vegetation is a mixture of shrubs, medium-sized trees (4.5 m) and tall grass (Supplemental Fig. S3). The maximum grass height can reach up to 2.5 m in the rainy season. The EC station at the cropland site is located in between the two other EC stations in a less populated area near the Burkinabe–Ghanaian border. A photo of this EC station with its surroundings is shown in Supplemental Fig. S4. The dominant crops in this plot are sorghum [*Sorghum bicolor* (L.) Moench], groundnut (*Arachis hypogaea* L.), and pearl millet [*Pennisetum glaucum* (L.) R. Br.]. After harvest, the site is mainly used for grazing by livestock. The maximum vegetation height is usually <1 m. A photo sequence in Fig. 8 illustrates the surrounding vegetation characteristics for the different seasons for the EC stations in Sumbrungu, Kayoro, and Nazinga. This sequence clearly shows the different vegetation structure and dynamics during the year between the different sites.

To ensure that long-term climate characteristics of the sites are comparable across the sites, the locations of the EC stations are approximately at the same latitude. The differences in

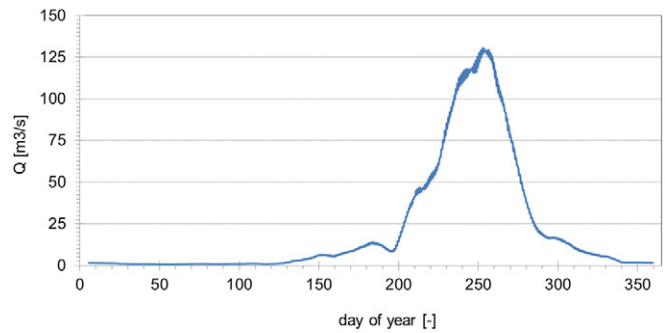


Fig. 7. The discharge ( $Q$ ) regime for the station Wiasi located at the outlet of the Sissili River basin based on daily measurements from 1960 to 2009.

precipitation characteristics that are important for the vegetation growth and dynamics, such as the annual precipitation amount or the onset of the rainy season, are therefore minor (Table 2). The soil texture of all EC sites is loamy sand or sandy loam, partially with a high proportion of coarse-grained materials (30%), for instance, in the top layer of the degraded site in Sumbrungu. The surrounding terrain of all EC stations is relatively flat with an estimated slope of <3° for each site. Further basic prerequisites for the site selection were a sufficient distance of the EC sites from nearby rivers or lakes (>200 m) and no groundwater or backwater influence in the analysis of the soil profile. Therefore, we assume that any influence from groundwater or backwater is relatively small for each site.

### Setup of the Eddy Covariance Stations

The EC station instrumentation is nearly identical for each site but with individual measurement heights. A schematic of the measurement devices of an EC station is presented in Fig. 9. This setup measures >20 variables at different height levels with a high temporal resolution (Table 3).

The core measurement devices of the EC stations are an open-path infrared gas analyzer (7500A, Li-COR) and a three-dimensional ultrasonic anemometer (CSAT3, Campbell). These devices measure atmospheric water vapor content, the atmospheric CO<sub>2</sub> content, and the horizontal and vertical wind components with a sampling frequency of 20 Hz. The measurement height of these devices is site dependent and varies between 2.65 m aboveground for the grassland site and 7.19 m aboveground for the near-natural site. The measurement height depends on the mean vegetation height within the fenced area of an EC station. Based on this setting, fluxes of sensible heat, latent heat, and CO<sub>2</sub> are calculated using the EC method (for further information regarding the application of this method, see Quansah et al., 2015), and references therein). The information from the three-dimensional sonic anemometer can also be used to determine total wind speed, total wind direction, and corresponding two-dimensional variables such as the horizontal wind speed and direction. Examples of the horizontal wind measurements from our EC stations are shown in Fig. 4.

Table 2. Site characteristics of the eddy covariance stations Nazinga, Kayoro, Sumbrungu, and Gorigo.

Characteristic†	Nazinga	Kayoro	Sumbrungu	Gorigo
Latitude, ° N	11.15156	10.91810	10.84660	10.94016
Longitude, ° W	-1.58570	-1.32090	-0.91740	-0.82644
Altitude, m	297	282	200	220
MAP, mm	994	960	978	(970)
ORS, date	5 May	5 May	5 May	(5 May)
CRS, date	18 Sept.	19 Sept.	21 Sept.	(20 Sept.)
DRS, d	137	138	140	(139)
Soil texture	Sandy loam	Loamy sand	Loamy sand	(Loamy sand)
Soil depth, cm	(>60)	(>65)	(50)	(>65)
Bedrock	amr‡	amr	amr	amr
Land use	Protected area	Cropland	Grassland	Grassland
Land use intensity	Very low	High	High	High
Max. grass height, m	2.5	1	0.1	0.1
Grass species§	<i>Ac, Ap, Hi</i>	<i>Aspp, Cspp</i>	<i>Ap, Bv, Sf</i>	<i>(Aspp, Bspp, Sspp)</i>
Crops¶	–	sh, gn, pm	–	–
Grazed by#	wh	dh	dh	dh
Grazing pressure	Very mild	Mild	Severe	Mild to severe
Tree layer	Discontinuous	Sparse	Sparse	Sparse
Tree species††	<i>Do, Ba, Id</i>	<i>Ad, Vp</i>	<i>Ad, Vp</i>	<i>Ad, Vp</i>
Mean tree height, m	(4,5)	(5)	(5)	(5)
Relief	Flat	Flat	Flat	Flat
Slope, °	(<3)	(<3)	(<3)	(<3)
Groundwater influence	(Small)	(Small)	(Small)	(Small)

† MAP, mean annual precipitation; ORS, onset of the rainy season; CRS, cessation of the rainy season; DRS, duration of the rainy season based on definitions from Odekunle (2004). For information about soil texture and soil chemistry we refer to Quansah et al. (2015). Information in parentheses are preliminary qualitative estimates (e.g., during site selection).

‡ amr, acidic metamorphic rocks.

§ *Ac, Andropogon chinensis; Ap, Andropogon pseudapricus; Hi, Hyparrhenia involucrate; Aspp, Andropogon spp.; Cspp, Cenchrus spp.; Bv, Brachiaria villosa; Sf, Spermocoe filifolia; Bspp, Brachiaria spp.; Sspp, Spermocoe spp.*

¶ sg, sorghum; gn, groundnut; pm, pearl millet.

# wh, wild herbivores; dm, domestic herbivores.

†† *Do, Daniellia oliveri; Ba, Burkea africana; Id, Isoberlinia doka; Ad, Adansonia digitate; Vp, Vitellaria paradoxa.*

A further important device of the EC stations is a net radiometer (CNR4, Kipp & Zonen) to determine the different radiation components of the energy balance and the total net radiation. The net radiometer consists of an upward- and downward-facing pair of pyranometers to measure the incoming and outgoing shortwave radiation (spectral range = 0.3–2 μm). In addition, a downward-facing pair of pyrgeometers is used to measure the longwave radiation exchanges (spectral range = 4.5–50 μm) between atmosphere and land surface. Since the incoming longwave radiation

cannot be measured directly, the longwave radiation components are obtained by correcting the radiation exchanges using the sensor temperature of the net radiometer.

By taking into consideration net radiation, the energy closure ratios (latent heat plus sensible heat vs. net radiation minus ground heat) of the EC stations' footprint areas are inspected, and fluxes of sensible and latent heat are validated. In addition, the measurements of the net radiometer are used to determine other important variables such as albedo, total net radiation, or net ecosystem exchanges onsite (Table 4). Examples of energy balance closures for the three EC stations are shown in Quansah et al. (2015) for the year 2013. This study showed a satisfying to very good energy balance closure indicated by a relatively high coefficient of determination ( $r^2 > 0.89$ ) between the sum of latent heat flux and sensible heat flux and the sum of net radiation minus ground heat flux. The analysis also revealed typical underestimations of the sum of heat fluxes ranging between 10 and 30% between the different sites, which was best for the near-natural site.

The EC stations also measure several standard meteorological variables. Air temperature and relative humidity are measured by a temperature and humidity probe (HMP155A, Campbell) using a ventilated radiation shield for protection. Like the anemometer and gas analyzer measurements, the air temperature and humidity measurements are taken at the same height and with the same frequency. The standard precipitation measurement set for each station consists of three independent devices with different measurement techniques: a weighing gauge (Pluvio2, Ott), a tipping bucket (52203, R. M. Young), and a disdrometer as part of a compact weather station (WXT 520, Vaisala). The weighing gauge is one of the most precise devices for measurements of point precipitation but is much more expensive than other devices. Thus, only the EC and the agrometeorological station were equipped with a weighing gauge and are used as reference for point precipitation measurements of the WASCAL

hydrometeorological observatory. In 2016, the standard precipitation measurement set for the EC station in Nazinga was extended with another disdrometer (OTT Parsivel sensor) to measure drop-size distribution and velocity of falling precipitation at a 2-m height.

An example of the hourly precipitation measurements from the weighing gauge and the disdrometer is shown for the EC station in Sumbrungu from October 2012 to November 2013 (Fig. 10). The sample consists of 508 joint wet observations where an hourly precipitation event was recorded at least at one measurement device.

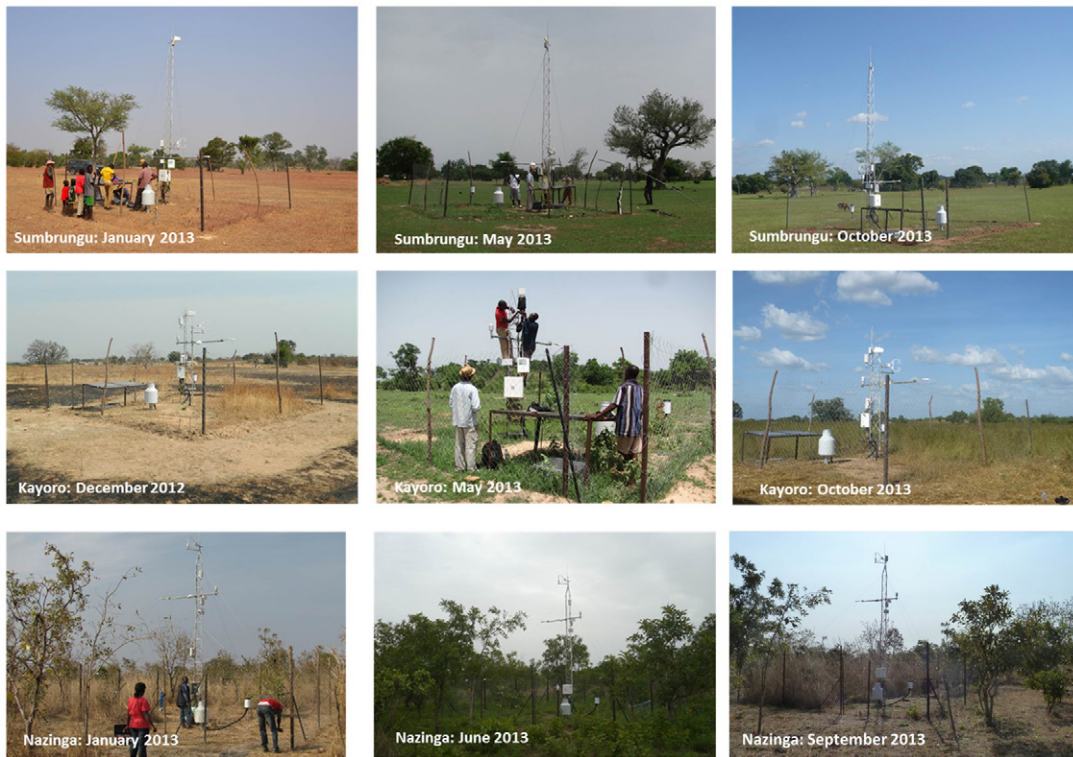


Fig. 8. The eddy covariance stations Nazinga (near-nature, protected wildlife area), Kayoro (cropland, grazed by livestock), and Sumbungu (strongly degraded grassland) during the dry season (December and January), onset (May and June), and cessation period of the rainy season (September and October). The photos were taken in 2012 and 2013.

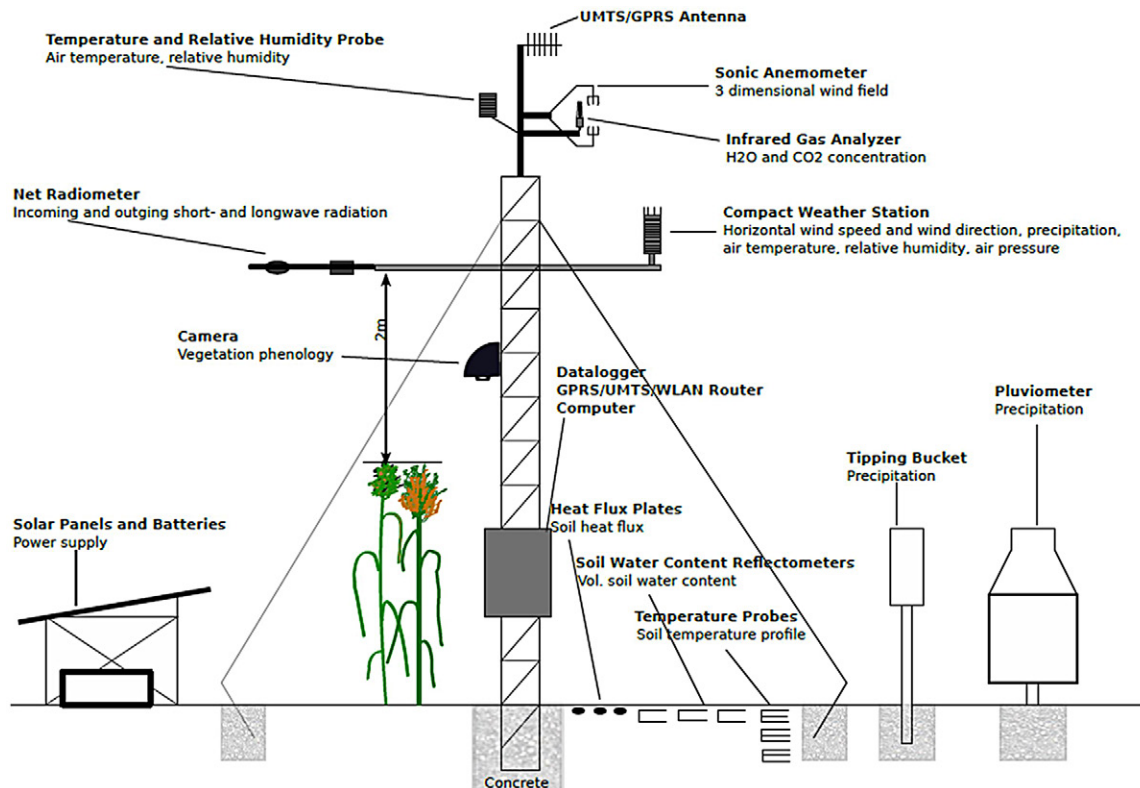


Fig. 9. An illustration of the components of an eddy covariance station including measurements variables and their corresponding devices (updated version from Bliefernicht et al., 2013).

Table 3. Basic measurement characteristics for the variables of the EC stations.

Variable	Characteristic†					
	T	H1	H2	H3	TR	SF
		m			min	Hz
Zonal wind component, $m s^{-1}$	Mean	2.65	3.15	7.19	30	20
Meridional wind component, $m s^{-1}$	Mean	2.65	3.15	7.19	30	20
Vertical wind component, $m s^{-1}$	Mean	2.65	3.15	7.19	30	20
Sonic (air) temperature, $^{\circ}C$	Mean	2.65	3.15	7.19	30	20
Atmospheric water vapor content, $g m^{-3}$	Mean	2.65	3.15	7.19	30	20
Atmospheric $CO_2$ content, $mg m^{-3}$	Mean	2.65	3.15	7.19	30	20
Air pressure, hPa	Mean	2.65	3.15	7.19	30	20
Longwave radiation exchange, surface–atmosphere, $W m^{-2}$	Mean	2.0	2.50	5.30	5‡	1/15
Incoming shortwave radiation, $W m^{-2}$	Mean	2.0	2.50	5.30	5‡	1/15
Longwave radiation exchange, surface–soil layer, $W m^{-2}$	Mean	2.0	2.50	5.30	5‡	1/15
Outgoing shortwave radiation, $W m^{-2}$	Mean	2.0	2.50	5.30	5‡	1/15
Air temperature, $^{\circ}C$	Mean	2.65	3.15	7.19	30	20
Relative humidity, %	Mean	2.65	3.15	7.19	30	20
Precipitation amount, mm	Sum	1.0	1.0	1.0	5‡	1/15
Precipitation amount, mm	Sum	1.0	1.0	1.0	5‡	1/15
Rainfall amount, mm	Sum	2.0	2.50	5.30	5‡	1/15
Hail amount, $hit cm^{-2}$	Sum	2.0	2.50	5.30	5‡	1/15
Air temperature, $^{\circ}C$	Mean	2.0	2.50	5.30	5‡	1/15
Horizontal wind speed, $m s^{-1}$	Mean	2.0	2.50	5.30	5‡	1/15
Horizontal wind direction, $^{\circ}$	Mean	2.0	2.50	5.30	5‡	1/15
Relative humidity, %	Mean	2.0	2.50	5.30	5‡	1/15
Air pressure, hPa	Mean	2.0	2.50	5.30	5‡	1/15
Soil temperature at 3 cm, $^{\circ}C$	Mean	0.03	0.03	0.03	5‡	1/15
Soil temperature at 10 cm, $^{\circ}C$	Mean	0.1	0.1	0.1	5‡	1/15
Soil temperature at 35 cm, $^{\circ}C$	Mean	0.35	0.35	0.35	5‡	1/15
Volumetric water content, %	Ensemble mean	0.03	0.03	0.03	5‡	1/15
Ground heat flux, $W m^{-2}$	Ensemble mean	0.08	0.08	0.08	5‡	1

† T, measurement type; H1, measurement height for Sumbrungu; H2, measurement height for Kayoro; H3, measurement height for Nazinga; TR, temporal resolution; SF, sampling frequency.

‡ TR was refined from 30 to 5 min over the first 2 yr.

The outcome shows a moderate to high correspondence between both measurement devices with a Spearman rank correlation coefficient ( $r_s$ ) of 0.69. Many data pairs are concentrated near the 1:1 line, in particular for the smaller precipitation amounts ( $<5 mm h^{-1}$ ). The total precipitation amounts recorded at the weighing gauge ( $P_t = 711 mm$ ) were slightly overestimated by the disdrometer (bias = 3.7%). Comparable results were obtained for the other sites for the same investigation period but with a lower correspondence at

Nazinga ( $r_s = 0.46$ ,  $P_t = 682 mm$ , bias = 2.2%) and a stronger over-estimation at Kayoro ( $r_s = 0.78$ ,  $P_t = 740 mm$ , bias 9.3%).

Each EC station also contains a low-cost compact weather station to measure five additional meteorological variables besides precipitation: air temperature, horizontal wind speed and direction, relative humidity, and air pressure. The measurements of this weather station are used as additional information for quality control and backup of meteorological measurements. The EC stations

Table 4. List of selected variables estimated and calculated at the eddy covariance station based on measurement variables listed in Table 3. In addition, the measurement heights of corresponding devices at Sumbrungu (H1), Kayoro (H2), and Nazinga (H3) are given.

Variable	Type	TR†	H1 H2 H3		
			min	m	
Sensible heat flux, $W m^{-2}$	Mean	30	2.65	3.15	7.19
Latent heat flux, $W m^{-2}$	Mean	30	2.65	3.15	7.19
Net ecosystem exchange, $W m^{-2}$	Mean	30	2.65	3.15	7.19
Absolute humidity, $g m^{-3}$	Mean	30	2.65	3.15	7.19
Net shortwave radiation, $W m^{-2}$	Mean	5‡	2.0	2.5	5.3
Net longwave radiation, $W m^{-2}$	Mean	5‡	2.0	2.5	5.3
Net total radiation, $W m^{-2}$	Mean	5‡	2.0	2.5	5.3
Albedo, %	Mean	5‡	2.0	2.5	5.3

† TR, temporal resolution.  
‡ TR was refined from 30 to 5 min over the first 2 yr.

are also equipped with several soil sensors. Ground heat fluxes are measured using three self-calibrating heat flux plates (HFP01SC, Hukseflux) side by side at 8-cm depth. In addition, vertical profiles of soil temperature are recorded at three different depths (3, 10, and 35 cm) using an averaging soil thermocouple probe (TCAV, Campbell). The soil moisture is recorded at 3-cm depth with soil water content reflectometers (CS616, Campbell). In addition, a web camera is installed at each EC station to observe its environment and, in particular, the vegetation. Two pictures of this webcam are shown for the EC station in Kayoro in Supplemental Fig. S5.

The surrounding area of each EC station is protected by a fence (~7 by 7 m) and a fire protection belt in the case of Kayoro and Nazinga. Each EC station is also equipped with two data loggers, a robust field computer and an automatic transmission unit with a universal mobile telecommunications system (UMTS) module. The field computer is needed to run the software for processing EC fluxes (Mauder and Foken, 2015) and for data archiving. The automatic data transmission to a data server hosted in Germany was tested continuously between 2012 and 2015 with daily data transfers from the EC stations. The power supply of each EC station consists of 2 solar panels with 190-W maximum power each, complemented by a pack of four 95-Ah batteries for nighttime measurements.

It is noted that the data coverage strongly varies between the different EC sites and also depend on the measurement variable. The data coverage was analyzed for the three EC sites from October 2012 to November 2016. It was poorest for Sumbrungu due to the thievery of equipment (see Technical Challenges below), which led to an interruption of the measurements for several weeks or longer. Approximately 68% of the nonturbulent fluxes and 51% of the turbulent fluxes are available for this site. Since the accessibility to the near-natural site in the Nazinga Game Ranch can be extremely challenging in the rainy season (see Technical Challenges), we lost

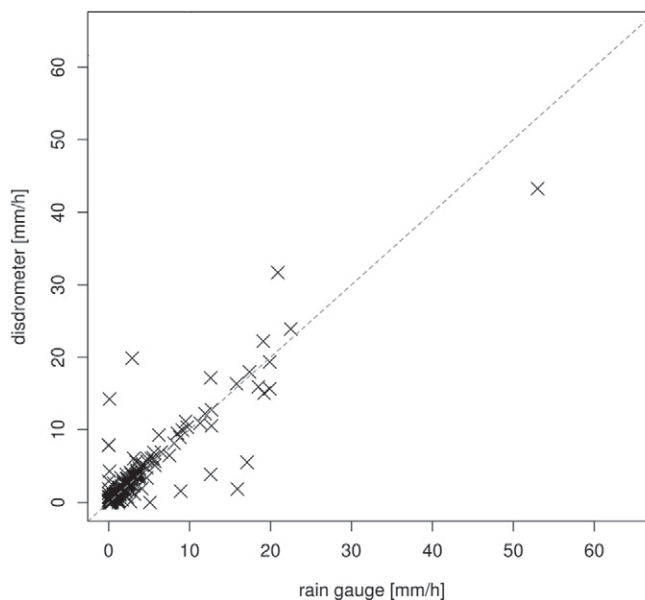


Fig. 10. Comparison of hourly precipitation measurements from weighing gauge and disdrometer for the measurement period from 9 Oct. 2012 to 27 Nov. 2013. The measurements are from the eddy covariance station in Sumbrungu. The total number of joint hourly observations was 508 where at least one device recorded a rainfall event. The total number of joint hourly observation with zeros on both measurement devices was 8010.

a larger amount of data several times due to systems failures. The data coverage was therefore only slightly better (5–10%) than at the Sumbrungu site. The best data coverage was obtained for the EC station in Kayoro, where ~90% of the nonturbulent fluxes and 72% of the turbulent fluxes were recorded.

### Characterizing the Representativeness of Eddy Covariance Measurements

Considerations regarding the representativeness of the EC measurements for their larger scale surroundings are based on Schmid (1997) and field experiences made, for example, by Mauder et al. (2007) during the NIMEX experiment. Schmid (1997) showed that the scale of the spatial average of each micrometeorological-point observation depends on several factors like meteorological conditions, measurement height, and the measured variable. Since measurement height and orientation of the equipment vary across the three EC sites (Table 3), the footprints of the EC station are site dependent and were set up to represent the site characteristics as well as possible under given circumstances and practical limitations.

Since the near-natural site is located in a dedicated area for research studies, anthropogenic activities are strongly reduced and vegetation disturbances due to human and wildlife activity are relatively small in this area. We therefore assume that the site properties within the fenced area are very similar to the site characteristics outside the fenced area of the EC site. However, this overall similarity within the EC fetch is disturbed through a fire protection belt (see section below), which is located outside the fence. The belt has a width of ~1.5 to 2.5 m, and it surrounds the

tower with a radius of  $\sim 5$  m. Given the net radiometer height of 5.3 m and the gas analyzer and sonic anemometer heights of 7.19 m, we assume that the radiation measurements are mainly affected by the area enclosed by the fire protection belt, whereas the flux footprint encompasses a larger area around the EC tower.

The EC site in Sumbrungu has no fire protection belt, since field burnings are prohibited in this densely populated area. Due to grazing activities, the vegetation within the fenced area can be different than in its surroundings. However, differences in vegetation height between both areas were comparably small, in contrast with the other sites, so we consider any impact on the radiation measurements and related quantities like the albedo to be small for this site.

At the EC site in Kayoro, footprints of measured variables are characterized by considerably more heterogeneous conditions, due to cropping activities outside the fence and densely growing weeds inside the fence, and a fire protection belt with similar dimensions as in Nazinga. However, we try to regularly cut down the vegetation during the growing season to keep the conditions as homogenous as possible. Moreover, Schmid (1997) recommended that under heterogeneous conditions, the EC equipment should be preferred over other micrometeorological equipment.

Given this straightforward qualitative description, we assume that the representativeness of the measurements is in an acceptable range for the EC sites in Nazinga and Sumbrungu, but much lower for the EC site in Kayoro. However, the impact of the fire protection belt and the lack of grazing and cropping activities within the fenced area should be addressed in future investigations, in combination with a detailed footprint analysis (Chen et al., 2009). Thus, our conclusions regarding the representativeness of measurements are tentative and should be taken with caution. However, it should be noted that the influence of grazing activities on the vegetation was analyzed nearby the EC sites in Sumbrungu and Nazinga within the last years. Moreover, the surroundings of the EC stations were monitored on a regular basis with a web camera (Supplemental Fig. S5). Thus, there are several options to get an estimate of the vegetation differences between the different areas of the EC fetch in the near future.

## Technical Challenges of Operating Eddy Covariance Stations and Other Equipment

Regular maintenance of the equipment can be highly challenging in this region, in particular when measurement devices are located in remote areas like the EC station in the protected area of the Nazinga Game Ranch. To reduce the number of maintenance trips, each EC station was equipped with a remote control software that allows us to check measurements, solve emergent software problems, and determine when the next maintenance trip to the station should be taken. The high standard of the mobile networks in Burkina Faso and Ghana with an almost country-wide coverage allowed remote access to the EC stations most of the time. Despite these achievements, regular onsite maintenance of the equipment is essential for minimizing measurement errors and equipment failures and for delivering high-quality data. The onsite maintenance of the

entire hydrometeorological equipment of the observation network was mainly done by a WASCAL technician based in the nearby Veia catchment in Bolgatanga. The technician was supported twice per year (before and after a rainy season) by doctoral or postdoctoral students due to the complexity of operating the EC stations. However, a “normal” onsite maintenance of the equipment was often challenging because of unforeseen problems that sometimes made maintenance trips to the stations impossible, such as cars getting stuck in the mud or breaking down, permanently flooded roads, or dangerous animals such as elephants and poisonous snakes, who use the surroundings (or even the equipment) as habitat.

A big safety problem for many meteorological stations in this region is wildfires, which are an essential element of the savanna systems in West Africa (Devineau et al., 2010). Field burnings are used by farmers to mineralize harvest residuals during the dry season. In addition, natural wildfires occur frequently in this region, even in protected areas like the Nazinga Game Ranch (Hema et al., 2017). To better protect the equipment from wildfires, the EC stations in Kayoro and Nazinga and several automatic weather stations are surrounded by a zone of  $\sim 1.5$ - to 2.5-m width where any vegetation is regularly shortened. Figure 11 and Supplemental Fig. S1 show the importance of these fire protection zones for the EC station in Kayoro. The photos were taken shortly after a field burning, which occurred in the November 2012, a few weeks after the installation of the EC station. The harvest residuals were completely burned by the fire, but thanks to the fire protection belt, no measurement devices were damaged.

A further challenging task is the protection of equipment against thievery and vandalism for the EC station in Sumbrungu. Particularly, solar panels and batteries are of high interest in this region due to the poor public power supply. Weather and EC stations are therefore located near households and dwellings ( $< 100$  m) away from main roads. In addition, guards of the nearby community are hired to watch the stations. This strategy works well for almost all stations, except for the EC station in Sumbrungu. The solar panels and the batteries of the EC station were stolen, leading to an interruption of the measurements for several weeks or more in 2014 and 2015, although this equipment was secured by a number of special security measures. In 2016, even the field computer was stolen from the EC station. Since the frequency and severity of the attempted thefts increased dramatically by the end of 2016, to a point that the guard was seriously injured, the station was relocated to another site in a less populated area of the Veia watershed.

## First Analysis of Radiation Fluxes and Albedo

Some basic analyses of the EC measurements are illustrated in Fig. 12 for the radiation fluxes. The upper panels of Fig. 12 show the diurnal cycle of the incoming and outgoing shortwave radiation for all three EC sites on a sunny day during the dry season. The incoming shortwave radiation measurements are almost identical for this day. However, the outgoing shortwave radiation of Sumbrungu is clearly higher in comparison with Nazinga, leading



Fig. 11. The photos show the eddy covariance (EC) station Kayoro and surroundings before (upper figures) and after wild-fire in November 2012 (lower figures). The upper photos were taken a few days after the implementation of the EC station in October 2012. The lower photos were taken on 2 Dec. 2012. The exact date and reason of the wildfire is unknown.

to higher albedo than at the other EC sites. Figure 12 also shows the annual cycle of the noon albedo for all three EC sites. The degraded grassland site has a clearly higher albedo than the other EC sites, resulting in much lower net radiation for this site.

### Data Management, Policy, and Products

The WASCAL database contains two different datasets from the hydrometeorological observatory of the Sissili and Vea watershed. These datasets consist of raw 5-min meteorological measurements from the network of automatic weather stations for seven variables

(Table 5). Since the raw data of the automatic weather stations and EC stations have gaps in the data, a second dataset was generated. This dataset consists of gap-filled, half-hourly time series for eight standard meteorological variables (Table 5). The measurements for the gap-filling were quality controlled by a comprehensive visual inspection (e.g., time series diagrams, scatterplots) and several quantitative methods like cross-comparison of basic univariate statistics and spatial correlograms. The data gaps were filled using a spatio-temporal infilling algorithm based on an inverse distance approach. This dataset was specifically generated as input information for the development and evaluation of land surface models such as the Noah Land Surface Model (Ek et al., 2003; Rosero et al., 2009). The

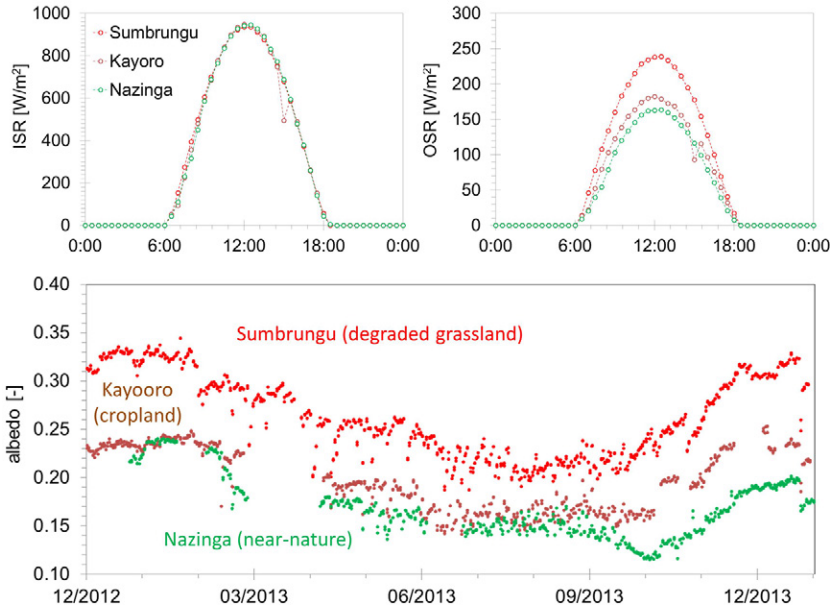


Fig. 12. Diurnal variation of the incoming (ISR) and outgoing shortwave radiation (OSR) of the eddy covariance (EC) stations Sumbrungu (strongly degraded grassland), Kayoro (cropland, grazed by livestock), and Nazinga (near-nature, protected wildlife area) for a sunny day, 19 Mar. 2013 (upper figures). Annual cycle of the noon albedo for the three EC stations (Sumbrungu, Kayoro, and Nazinga) for the year 2013 (lower figure).

Table 5. List of variables provided by the West African Science Service Centre on Climate Change and Adapted Land Use (WASCAL) database via two different datasets: “original” and “gap-free.”

Variable	Type	Original			Gap-free		
		TR†	WS‡	EC§	TR	WS	EC
		min			min		
Incoming shortwave radiation, $W m^{-2}$	Mean	5	o¶	-#	30	o	o
Incoming longwave radiation, $W m^{-2}$	Mean	-	-	-	30	-	o
Air temperature, °C	Mean	5	o	-	30	o	o
Horizontal wind direction, °	Mean	5	o	-	-	-	-
Horizontal wind speed, $m s^{-1}$	Mean	5	o	-	30	o	o
Relative humidity, %	Mean	5	o	-	-	-	-
Specific humidity, $g kg^{-1}$	Mean	-	-	-	30	o	o
Air pressure, hPa	Mean	5	o	-	-	-	-
Mean sea level pressure, hPa	Mean	-	-	-	30	o	o
Precipitation amount, mm	Sum	5	o	-	30	o	o

† TR, temporal resolution.  
‡ WS, automatic weather station.  
§ EC, eddy covariance station.  
¶ o, data are available.  
# -, data are not available.

dataset is available for the period from 1 Jan. 2013 to 31 Dec. 2013 for most of the automatic weather stations and for the three EC stations. Please note that the current WASCAL database also includes further hydrometeorological datasets like the measurements from the other two hydrometeorological observatories of the Dana watershed in Southwest Burkina Faso and the Dassari watershed in North Benin.

Moreover, the datasets from the WASCAL hydrometeorological observatory are complemented by several other high-resolution climate datasets, which were recently established as basic data for improved climate analysis. These datasets include a gridded daily precipitation dataset for Burkina Faso, Ghana, and Benin based on long-term daily time series from >300 rainfall stations. This dataset ranges from 1970 to 2010 and has a spatial resolution of ~10 km. In addition, a number of gridded subdaily meteorological datasets from two high-resolution RCM simulations driven by reanalysis data are available for a recent period (e.g., 1980–2010). These products are based on two RCMs, which have been specifically tested and evaluated for the region of West Africa (Klein et al., 2015; Dieng et al., 2017). The meteorological datasets have a spatial resolution of ~12 km and cover the entire West African continent. The RCMs were also used to produce an ensemble of high-resolution (~12 km) regional climate scenarios for a historical period (1980–2010) and two future time periods (e.g., 2020–2050, 2070–2100) for West Africa (Dieng et al., 2018; Heinzeller et al., 2018). More detailed information regarding these datasets is given on the corresponding website of the WASCAL database and in Heinzeller et al. (2018). The datasets and derived products are

either open access or accessible on request to the data authors at the WASCAL Data Discovery Portal: [https://wascal-dataportal.org/wascal\\_searchportal2/](https://wascal-dataportal.org/wascal_searchportal2/). The data from the hydrometeorological observatory are managed and owned by WASCAL and can be provided for a period ranging from the start of the measurements to today.

### New Insights and Scientific Findings

A novel hydrometeorological observatory was established for the West African Sudan Savanna for the Sissili and Vea basin. A unique element of this observatory is a micrometeorological experiment to quantify the impact of land cover changes on water, energy, and CO<sub>2</sub> fluxes. Although many challenges had to be mastered during the last years, the data analysis from the micrometeorological field experiment revealed a satisfying to very good estimation of energy and water fluxes (Quansah et al., 2015). In the study of Quansah et al. (2015), we also indicated that the West African Sudan Savannah’s C-storage function is completely outweighed by great C losses when the site is intensively used for farming. Since this analysis was performed for only 1 yr, future studies must confirm these findings.

Data from the EC stations are also used for an evaluation of land–atmosphere exchange processes simulated by land surface models (Quansah et al., 2017) or by coupled RCMs such as WRF-Hydro. Recently, new WRF-Hydro simulations were performed for a period of 4 yr (2013–2016) following Arnault et al. (2016) and Naabil et al. (2017). The model performance of the WRF-Hydro simulations is shown in Fig. 13 for the heat and radiation fluxes of the EC station in Kayoro. The diagram indicates high skill for the simulation of the radiation fluxes and sensible heat. The WRF-Hydro simulations even maintain a moderate quality for latent heat fluxes during several months. The simulation of this variable is considered highly challenging, even for land surface models under perfect boundary conditions, as illustrated in Hogue et al. (2005).

### Future Challenges and Perspectives

Despite numerous achievements being made since the initiation of the observatory, there are still several challenges that need to be addressed in the near future. A highly important step is the improvement of the current facilities of the observatory like automatic data transfer and quality control. Although this was demonstrated for the EC stations in the last years, it also needs to be established for the automatic weather stations and other field equipment. This is essential for a rapid identification of system failures and for establishing a continuous data transfer to the WASCAL database for providing high-quality measurements in real time. A further important task

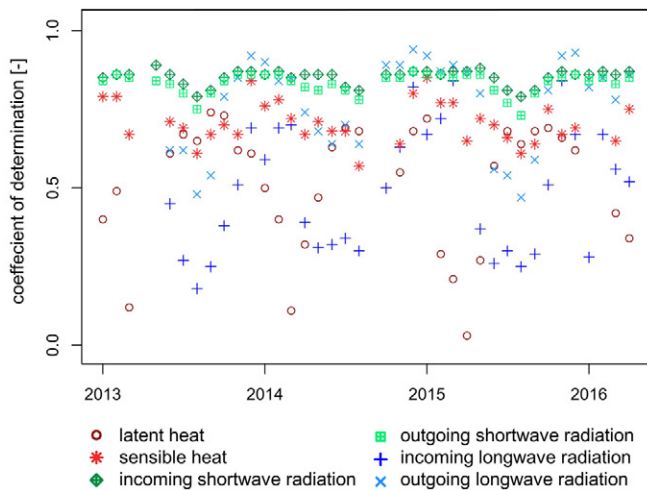


Fig. 13. Monthly performance of the hydrologically enhanced version of the Weather and Research Forecasting Model (WRF-Hydro) for shortwave and longwave radiation and heat fluxes for the eddy covariance station Kayoro from 2013 to 2016. The coefficient of determination is selected as performance measure to illustrate how much of the observed variability is explained by the model simulations.

is the improvement of the provision of datasets for research studies conducted in this region. Although a wide range of variables are measured by the observatory, data requirements of interdisciplinary studies often differ from hydrometeorological investigations, and individual solutions are therefore needed. An improved provisioning process will facilitate data use and will make the dataset of the observatory a unique source of information for a much broader research community. A further challenge is the analysis of the EC measurements. So far, only the CO<sub>2</sub> fluxes for the year 2013 were analyzed in detail. Current and future research activities should therefore focus on the analysis of all EC measurements to confirm the findings of Quansah et al. (2015) and to perform a much more detailed analysis of the water and energy fluxes as presented in their study.

The datasets provided by the observatory are needed for various long-term field experiments and several advanced modeling studies for improved analysis of climate and land use changes in the West African Sudan Savanna (Poméon et al., 2018). They can also be used as ground truth for evaluation of remote sensing products and climate model output products (Decker et al., 2012). The dataset provides useful information for large-scale meteorological field campaigns performed, for example, in Dynamics–Aerosol–Chemistry–Cloud Interactions in West Africa (DACCIIWA; Knippertz et al., 2015) for a better scientific understanding of monsoon processes and feedback mechanisms in this region. The observatory also forms an excellent platform for future studies that use not only the available observational data, but also extend the current facilities of the observatory for short-term field campaigns or as long-term experiments with additional measurement equipment. The hydrometeorological observatory can also serve as an observational foundation for the establishment of cutting-edge, long-term environmental observatories that allows for improved

interdisciplinary analysis of environmental changes and their socioeconomic impacts on the savanna regions of West Africa.

In addition, a large-scale meteorological observation network is currently established by WASCAL. As a transboundary network, it is shared and integrated into the national observational networks of the different national meteorological and hydrological services of the West African countries (Salack et al., 2018b). This new network will extend the capacities of the WASCAL hydrometeorological observatories in the West African Sudan Savanna to deliver a new generation of hydrometeorological data products for an improved monitoring of climate extremes and for an in-depth analysis of climate and land use changes in this region.

## Supplemental Material

The supplemental material shows additional pictures of the EC stations in Nazinga, Kayoro, and Sumbrungu to better illustrate the differences between the EC sites (near-nature, cropland, and degraded grassland). We also show photos from the new EC station in Gorigo (degraded grassland) established in May 2017 and from the webcam for the EC station Kayoro after the field burning in December 2012. In addition, meta-information like geographical coordinates are listed for the meteorological stations installed for the WASCAL observatory.

## Acknowledgments

This work was part of the WASCAL ([www.wascal.org](http://www.wascal.org)) program funded by the Federal Ministry of Education and Research in Germany (Grant nos. 01LG1202C and 01LG1202C1). We also want to acknowledge the meteorological and hydrological services of Burkina Faso and Ghana for providing the hydrometeorological data and three anonymous reviewers for their valuable comments.

## References

- Adongo, T.A., J.X. Kugbe, and V.D. Gbedzi. 2014. Siltation of the reservoir of Veia irrigation dam in the Bongo District of the Upper East Region, Ghana. *Int. J. Sci. Technol.* 4(12).
- Arnault, J., L. Hingerl, A. Aduna, S. Andresen, J. Bliefernicht, T. Rummeler, and H. Kunstmann. 2014. Evaluation of a fully coupled atmospheric-hydrological modeling system for the Sissili watershed in the West African Sudanian Savannah. In: B. Fersch et al., editors, *Book of abstracts of the 1st European Fully Coupled Atmospheric-Hydrological Modeling and WRF-Hydro Users Workshop*, Cosenza, Italy. 11–13 June 2014. Univ. of Calabria, Rende, Italy. p. 35–39.
- Arnault, J., S. Wagner, R. Rummeler, B. Fersch, J. Bliefernicht, S. Andresen, and H. Kunstmann. 2016. Role of runoff-infiltration partitioning and resolved overland flow on land-atmosphere feedbacks: A case-study with the WRF-Hydro coupled modeling system for West Africa. *J. Hydrometeorol.* 17:1489–1516. doi:10.1175/JHM-D-15-0089.1
- Baldocchi, D., E. Falge, L. Gu, R. Olson, D. Hollinger, S. Running, and S. Wofsy. 2001. FLUXNET: A new tool to study the temporal and spatial variability of ecosystem-scale carbon dioxide, water vapor, and energy flux densities. *Bull. Am. Meteorol. Soc.* 82:2415–2434. doi:10.1175/1520-0477(2001)082<2415:FANTTS>2.3.CO;2
- Barry, B., E. Obuobie, M. Andreini, W. Andah, and M. Pluquet. 2005. The Volta river basin: Comparative study of river basin development and management. *Int. Water Manage. Inst., Comprehensive Assess. Water Manage. Agric.*, Colombo, Sri Lanka.
- Blanc, J.J., R.F.W. Barnes, G.C. Craig, H.T. Dublin, C.R. Thouless, I. Douglas-Hamilton, and J.A. Hart. 2007. African elephant status report 2007: An update from the African Elephant Database. *Occasional Paper Ser. IUCN Species Survival Comm.*, No. 33. IUCN/SSC African Elephant Specialist Group. *Int. Union Conserv. Nat.*, Gland, Switzerland.
- Bliefernicht, J., K. Kunstmann, L. Hingerl, T. Rummeler, U. Gessner, S. Andresen, et al. 2013. Field and simulation experiments for investigating regional land-atmosphere interactions in West Africa: Experimental setup and first results. In: E. Boegh, et al., editors, *Climate and land surface changes in hydrology*. RedBook Ser. 359. *Int. Assoc. Hydrol. Sci.*, London. p. 226–232.

- Blöschl, G., A.P. Blaschke, M. Broer, C. Bucher, G. Carr, X. Chen, and P. Haas. 2016. The Hydrological Open Air Laboratory (HOAL) in Petzenkirchen: A hypothesis-driven observatory. *Hydrol. Earth Syst. Sci.* 20:227–255. doi:10.5194/hess-20-227-2016
- Bogena, H., R. Kunkel, T. Pütz, H. Vereecken, E. Krüger, S. Zacharias, and H.P. Schmid. 2012. TERENO: Long-term monitoring network for terrestrial environmental research. *Hydrol. Wasserbewirtschaft.* 56:138–143.
- Boudevillain, B., G. Delrieu, B. Galabertier, L. Bonnifait, L. Bouilloud, P.E. Kirstetter, and M.L. Mosini. 2011. The Cévennes-Vivarais Mediterranean Hydrometeorological Observatory database. *Water Resour. Res.* 47:W07701. doi:10.1029/2010WR010353
- Butts, M., M. Drews, M.A. Larsen, S. Lerer, S.H. Rasmussen, J. Grooss, and J.H. Christensen. 2014. Embedding complex hydrology in the regional climate system: Dynamic coupling across different modelling domains. *Adv. Water Resour.* 74:166–184. doi:10.1016/j.advwatres.2014.09.004
- Cappelaere, B., L. Descroix, T. Lebel, N. Boulain, D. Ramier, J.P. Laurent, and V. Chaffard. 2009. The AMMA-CATCH experiment in the cultivated Sahelian area of south-west Niger: Investigating water cycle response to a fluctuating climate and changing environment. *J. Hydrol.* 375:34–51. doi:10.1016/j.jhydrol.2009.06.021
- Ciais, P., A. Bombelli, M. Williams, S.L. Piao, J. Chave, C.M. Ryan, and R. Valentini. 2011. The carbon balance of Africa: Synthesis of recent research studies. *Philos. Trans. R. Soc., A* 369:2038–2057. doi:10.1098/rsta.2010.0328
- Chen, B., T.A. Black, N.C. Coops, and K. Morgenstern. 2009. Assessing tower flux footprint climatology and scaling between remotely sensed and eddy covariance measurements. *Boundary-Layer Meteorol.* 130:137–167. doi:10.1007/s10546-008-9339-1
- Danso, I., T. Gaiser, H. Webber, J. Naab, and F. Ewert. 2018. Response of maize to different nitrogen application rates and tillage practices under two slope positions in the face of current climate variability in the Sudan Savanna of West Africa. In: O. Saito, et al., editors, *Strategies for building resilience against climate and ecosystem changes in sub-Saharan Africa*. Springer, Singapore. p. 41–58. doi:10.1007/978-981-10-4796-1\_3
- Decker, M., M.A. Brunke, Z. Wang, K. Sakaguchi, X. Zeng, and M.G. Bosilovich. 2012. Evaluation of the reanalysis products from GSFC, NCEP, and ECMWF using flux tower observations. *J. Clim.* 25:1916–1944. doi:10.1175/JCLI-D-11-00004.1
- Delrieu, G., J. Nicol, E. Yates, P.-E. Kirstetter, J.-D. Creutin, S. Anquetin, et al. 2005. The catastrophic flash-flood event of 8-9 September 2002 in the Gard Region, France: A first case study for the Cévennes-Vivarais Mediterranean Hydrometeorological Observatory. *J. Hydrometeorol.* 6:34–52. doi:10.1175/JHM-400.1
- Devineau, J.L., A. Fournier, and S. Nignan. 2010. Savanna fire regimes assessment with MODIS fire data: Their relationship to land cover and plant species distribution in western Burkina Faso (West Africa). *J. Arid Environ.* 74:1092–1101. doi:10.1016/j.jaridenv.2010.03.009
- Dieng, D., G. Smiatek, J. Bliefernicht, D. Heinzeller, A. Sarr, A.T. Gaye, and H. Kunstmann. 2017. Evaluation of the COSMO-CLM high-resolution climate simulations over West Africa. *J. Geophys. Res. Atmos.* 122:1437–1455. doi:10.1002/2016JD025457
- Dieng, D.B., P. Laux, G. Smiatek, D. Heinzeller, J. Bliefernicht, H.G. Kunstmann, et al. 2018. Performance analysis and projected changes of agro-climatological indices across West Africa based on high-resolution regional climate model simulations. *J. Geophys. Res. Atmos.* 123:7950–7973. doi:10.1029/2018JD028536
- Dietz, T., D. Millar, S. Dittoh, F. Obeng, and E. Ofori-Sarpong. 2004. Climate and livelihood change in North East Ghana. In: A.J. Dietz, et al., editors, *The impact of climate change on drylands*. Springer, Dordrecht, the Netherlands. p. 149–172. doi:10.1007/1-4020-2158-5\_12
- Dimobe, K., D. Goetze, A. Ouédraogo, G. Forkuor, K. Wala, S. Porembski, and A. Thiombiano. 2017. Spatio-temporal dynamics in land use and habitat fragmentation within a protected area dedicated to tourism in a Sudanian Savanna of West Africa. *J. Landscape Ecol.* 10:75–95. doi:10.1515/jlecol-2017-0011
- Dimobe, K., A. Ouédraogo, S. Soma, D. Goetze, S. Porembski, and A. Thiombiano. 2015. Identification of driving factors of land degradation and deforestation in the wildlife reserve of Bontioli (Burkina Faso, West Africa). *Global Ecol. Conserv.* 4:559–571. doi:10.1016/j.gecco.2015.10.006
- Dinye, R.D., and J. Ayitio. 2013. Irrigated agricultural production and poverty reduction in Northern Ghana: A case study of the Tono irrigation scheme in the Kassena Nankana district. *Int. J. Water Resour. Environ. Eng.* 5:119–133.
- Durre, I., M.J. Menne, B.E. Gleason, T.G. Houston, and R.S. Vose. 2010. Comprehensive automated quality assurance of daily surface observations. *J. Appl. Meteorol. Climatol.* 49:1615–1633. doi:10.1175/2010JAMC2375.1
- Ek, M.B., K.E. Mitchell, Y. Lin, E. Rogers, P. Grunmann, V. Koren, and J.D. Tarpley. 2003. Implementation of Noah land surface model advances in the National Centers for Environmental Prediction operational meso-scale Eta model. *J. Geophys. Res.* 108:8851. doi:10.1029/2002JD003296
- Engel, T., A.H. Fink, P. Knippertz, G. Pante, and J. Bliefernicht. 2017. Extreme precipitation in the West African cities of Dakar and Ouagadougou: Atmospheric dynamics and implications for flood risk assessments. *J. Hydrometeorol.* 18:2937–2957. doi:10.1175/JHM-D-16-0218.1
- Ferner, J., A. Linstädter, K.H. Südekum, and S. Schmidlein. 2015. Spectral indicators of forage quality in West Africa's tropical savannas. *Int. J. Appl. Earth Obs. Geoinf.* 41:99–106. doi:10.1016/j.jag.2015.04.019
- Fleury, L., J.-L. Boichard, G. Brissebrat, S. Cloché, L. Eymard, L. Mastrorillo, O. Moulaye, et al. 2011. AMMA information system: An efficient cross-disciplinary tool and a legacy for forthcoming projects. *Atmos. Sci. Lett.* 12:149–154. doi:10.1002/asl.303
- FLUXNET. 2018. A global network: Site summary. FLUXNET. <http://fluxnet.fluxdata.org/sites/site-summary> (accessed 30 Mar. 2018).
- Forkuor, G., C. Conrad, M. Thiel, B.J.-B. Zougrana, and J.E. Tondoh. 2017. Multiscale remote sensing to map the spatial distribution and extent of cropland in the Sudanian Savanna of West Africa. *Remote Sens.* 9:839. doi:10.3390/rs9080839
- Fowe, T., H. Karambiri, J.E. Paturel, J.C. Poussin, and P. Cecchi. 2015. Water balance of small reservoirs in the Volta basin: A case study of Boura reservoir in Burkina Faso. *Agric. Water Manage.* 152:99–109. doi:10.1016/j.agwat.2015.01.006
- Gash, J.H.C., P. Kabat, B.A. Monteny, M. Amadou, P. Bessemoulin, H. Billing, and C.J. Holwill. 1997. The variability of evaporation during the HAPEX-Sahel intensive observation period. *J. Hydrol.* 188–189:385–399. doi:10.1016/S0022-1694(96)03167-8
- Gessner, U., K. Knauer, C. Kuenzer, and S. Dech. 2015. Land surface phenology in a West African savanna: Impact of land use, land cover and fire. In: C. Kuenzer, et al., editors, *Remote sensing time series, remote sensing and digital image processing*. Springer, Cham, Switzerland. p. 203–223. doi:10.1007/978-3-319-15967-6\_10
- Gochis, D.J., W. Yu, and D.N. Yates. 2013. The WRF-Hydro model technical description and user's guide. Version 1.0. Natl. Ctr. Atmos. Res., Boulder, CO.
- Goutorbe, J.P., T. Lebel, A. Tinga, P. Bessemoulin, J. Brouwer, A.J. Dolman, and Y.H. Kerr. 1994. HAPEX-Sahel: A large-scale study of land-atmosphere interactions in the semi-arid tropics. *Ann. Geophys.* 12:53–64. doi:10.1007/s00585-994-0053-0
- Green, J.K., A.G. Konings, S.H. Alemohammad, J. Berry, D. Entekhabi, J. Kolassa, et al. 2017. Regionally strong feedbacks between the atmosphere and terrestrial biosphere. *Nat. Geosci.* 10:410–414. doi:10.1038/ngeo2957
- Guuroh, R.T., J.C. Ruppert, J. Ferner, K. Čanak, S. Schmidlein, and A. Linstädter. 2018. Drivers of forage provision and erosion control in West African savannas: A macroecological perspective. *Agric. Ecosyst. Environ.* 251:257–267. doi:10.1016/j.agee.2017.09.017
- Guyot, A., J.M. Cohard, S. Anquetin, S. Galle, and C.R. Lloyd. 2009. Combined analysis of energy and water budgets to consolidate latent heat flux estimation using an infrared scintillometer. *J. Hydrol.* 375:227–240. doi:10.1016/j.jhydrol.2008.12.027
- Heinzeller, D., D. Dieng, G. Smiatek, C. Olusegun, C. Klein, I. Hamann, et al. 2018. The WASCAL high-resolution regional climate simulation ensemble for West Africa: Concept, dissemination, assessment. *Earth Syst. Sci. Data* 10:815–835. doi:10.5194/essd-10-815-2018
- Hema, E.M., R.F. Barnes, and W. Guenda. 2011. Distribution of savannah elephants (*Loxodonta africana* Blumenbach 1797) within Nazinga Game Ranch, Southern Burkina Faso. *Afr. J. Ecol.* 49:141–149. doi:10.1111/j.1365-2028.2010.01239.x
- Hema, E.M., M. Di Vittorio, R.F. Barnes, W. Guenda, and L. Luiselli. 2017. Detection of interannual population trends in seven herbivores from a

- West African savannah: A comparison between dung counts and direct counts of individuals. *Afr. J. Ecol.* 55:609–617. doi:10.1111/aje.12397
- Hingerl, L., H. Kunstmann, S. Wagner, M. Mauder, J. Bliefernicht, and R. Rigon. 2016. Spatio-temporal variability of water and energy fluxes: A case study for a mesoscale catchment in pre-alpine environment. *Hydrol. Processes* 30:3804–3823. doi:10.1002/hyp.10893
- Hogue, T.S., L. Bastidas, H. Gupta, S. Sorooshian, K. Mitchell, and W. Emmerich. 2005. Evaluation and transferability of the Noah land surface model in semiarid environments. *J. Hydrometeorol.* 6:68–84. doi:10.1175/JHM-402.1
- Jachmann, H. 1991. Evaluation of four survey methods for estimating elephant densities. *Afr. J. Ecol.* 29:188–195. doi:10.1111/j.1365-2028.1991.tb01001.x
- Jachmann, H., and T. Croes. 1991. Effects of browsing by elephants on the *Combretum/Terminalia* woodland at the Nazinga Game Ranch, Burkina Faso, West Africa. *Biol. Conserv.* 57:13–24. doi:10.1016/0006-3207(91)90105-1
- Jegede, O.O., M. Mauder, E.C. Okogbue, T. Foken, E.E. Balogun, J.A. Adedokun, et al. 2004. The Nigerian Micrometeorological Experiment (NIMEX-1): An overview. *Ife J. Sci.* 6:191–202. doi:10.4314/ijfs.v6i2.32147
- Jensen, J.K., and P. Engesgaard. 2011. Nonuniform groundwater discharge across a streambed: Heat as a tracer. *Vadose Zone J.* 10:98–109. doi:10.2136/vzj2010.0005
- Jensen, K.H., and T.H. Illangasekare. 2011. HOBE: A hydrological observatory. *Vadose Zone J.* 10:1–7. doi:10.2136/vzj2011.0006
- Jones, L., A. Dougill, R.G. Jones, A. Steynor, P. Watkiss, C. Kane, and J.P. Roux. 2015. Ensuring climate information guides long-term development. *Nat. Clim. Change* 5:812–814. doi:10.1038/nclimate2701
- Kahan, D.S., Y. Xue, and S.J. Allen. 2006. The impact of vegetation and soil parameters in simulations of surface energy and water balance in the semi-arid Sahel: A case study using SEBEX and HAPEX-Sahel data. *J. Hydrol.* 320:238–259. doi:10.1016/j.jhydrol.2005.07.011
- Kiese, R., B. Fersch, C. Baeßler, C. Brosy, K. Butterbach-Bahl, C. Chwala, et al. 2018. The TERENO Pre-Alpine Observatory: Integrating meteorological, hydrological, and biogeochemical measurements and modeling. *Vadose Zone J.* 17:180060. doi:10.2136/vzj2018.03.0060
- Klein, C., J. Bliefernicht, D. Heinzeller, U. Gessner, I. Klein, and H. Kunstmann. 2017. Feedback of interannual vegetation change: A regional climate model analysis for the West African monsoon. *Clim. Dyn.* 48:2837–2858. doi:10.1007/s00382-016-3237-x
- Klein, C., D. Heinzeller, J. Bliefernicht, and H. Kunstmann. 2015. Variability of West African monsoon patterns generated by a WRF multi-physics ensemble. *Clim. Dyn.* 45:2733–2755. doi:10.1007/s00382-015-2505-5
- Knauer, K., U. Gessner, R. Fensholt, G. Forkuor, and C. Kuenzer. 2017. Monitoring agricultural expansion in Burkina Faso over 14 years with 30 m resolution time series: The role of population growth and implications for the environment. *Remote Sens.* 9:132. doi:10.3390/rs9020132
- Knauer, K., U. Gessner, R. Fensholt, and C. Kuenzer. 2016. An ESTARFM fusion framework for the generation of large-scale time series in cloud-prone and heterogeneous landscapes. *Remote Sens.* 8:425. doi:10.3390/rs8050425
- Knippertz, P., H. Coe, J.C. Chiu, M.J. Evans, A.H. Fink, N. Kalthoff, et al. 2015. The DACCIWA Project: Dynamics–aerosol–chemistry–cloud interactions in West Africa. *Bull. Am. Meteorol. Soc.* 96:1451–1460. doi:10.1175/BAMS-D-14-00108.1
- Koch, J., T. Cornelissen, Z. Fang, H. Bogen, B. Diekkrüger, S. Kollet, and S. Stisen. 2016. Inter-comparison of three distributed hydrological models with respect to seasonal variability of soil moisture patterns at a small forested catchment. *J. Hydrol.* 533:234–249. doi:10.1016/j.jhydrol.2015.12.002
- Koffi, K.V., E. Obuobie, A. Banning, and S. Wohnlich. 2017. Hydrochemical characteristics of groundwater and surface water for domestic and irrigation purposes in Vea catchment, Northern Ghana. *Environ. Earth Sci.* 76:185. doi:10.1007/s12665-017-6490-3
- Krieg, J., D. Goetze, S. Porembski, P. Arnold, K.E. Linsenmair, and K. Stein. 2017. Floral and reproductive biology of *Moringa oleifera* (Moringaceae) in Burkina Faso, West Africa. *Acta Hort.* 1158:63–70. doi:10.17660/ActaHortic.2017.1158.8
- Kunkel, R., J. Sorg, R. Eckardt, O. Kolditz, K.H. Rink, and H. Vereecken. 2013. TEODOOR: A distributed geodata infrastructure for terrestrial observation data. *Environ. Earth Sci.* 69:507–521. doi:10.1007/s12665-013-2370-7
- Larsen, M.A.D., J.C. Refsgaard, M. Drews, M.B. Butts, K.H. Jensen, J.H. Christensen, and O.B. Christensen. 2014. Results from a full coupling of the HIRHAM regional climate model and the MIKE SHE hydrological model for a Danish catchment. *Hydrol. Earth Syst. Sci.* 18:4733–4749. doi:10.5194/hess-18-4733-2014
- Laux, P., H. Kunstmann, and A. Bárdossy. 2008. Predicting the regional onset of the rainy season in West Africa. *Int. J. Climatol.* 28:329–342. doi:10.1002/joc.1542
- Le Lay, M., G.M. Saulnier, S. Galle, L. Séguis, M. Métadier, and C. Peugeot. 2008. Model representation of the Sudanian hydrological processes: Application on the Donga catchment (Benin). *J. Hydrol.* 363:32–41. doi:10.1016/j.jhydrol.2008.09.006
- Lebel, T., B. Cappelraere, S. Galle, N. Hanan, L. Kergoat, S. Levis, and C. Peugeot. 2009. AMMA-CATCH studies in the Sahelian region of West-Africa: An overview. *J. Hydrol.* 375:3–13. doi:10.1016/j.jhydrol.2009.03.020
- Lebel, T., H. Sauvageot, M. Hoepffner, M. Desbois, B. Guillot, and P. Hubert. 1992. Rainfall estimation in the Sahel: The EPSAT-NIGER experiment. *Hydrol. Sci. J.* 37:201–215. doi:10.1080/02626669209492582
- Lebel, T., J.D. Taupin, and N. d'Amato. 1997. Rainfall monitoring during HAPEX-Sahel. 1. General rainfall conditions and climatology. *J. Hydrol.* 188–189:74–96. doi:10.1016/S0022-1694(96)03155-1
- Liebe, J., N. van de Giesen, and M. Andreini. 2005. Estimation of small reservoir storage capacities in a semi-arid environment: A case study in the Upper East Region of Ghana. *Phys. Chem. Earth Parts ABC* 30:448–454. doi:10.1016/j.pce.2005.06.011
- Marchal, A., P. Lejeune, P. Bouché, M. Ouédraogo, P. Sawadogo, D.D. Yaméogo, and C. Vermeulen. 2012. Status of medium-sized ungulate populations in 2010, at the Nazinga Game Ranch, Burkina Faso (Western Africa). *Biotechnol. Agron. Soc. Environ.* 16:307.
- Masih, I., S. Maskey, F.E.F. Mussá, and P. Trambauer. 2014. A review of droughts on the African continent: A geospatial and long-term perspective. *Hydrol. Earth Syst. Sci.* 18:3635–3649. doi:10.5194/hess-18-3635-2014
- Mauder, M., M. Cuntz, C. Drüe, A. Graf, C. Rebmann, H.P. Schmid, et al. 2013. A strategy for quality and uncertainty assessment of long-term eddy-covariance measurements. *Agric. Forest Meteorol.* 169:122–135. doi:10.1016/j.agrformet.2012.09.006
- Mauder, M., and T. Foken. 2015. Documentation and instruction manual of the eddy-covariance software package TK3 (update). Univ. Bayreuth, Bayreuth, Germany.
- Mauder, M., O.O. Jegede, E.C. Okogbue, F. Wimmer, and T. Foken. 2007. Surface energy balance measurements at a tropical site in West Africa during the transition from dry to wet season. *Theor. Appl. Climatol.* 89:171–183. doi:10.1007/s00704-006-0252-6
- Menne, M.J., I. Durre, R.S. Vose, B.E. Gleason, and T.G. Houston. 2012. An overview of the global historical climatology network-daily database. *J. Atmos. Ocean. Technol.* 29:897–910. doi:10.1175/JTECH-D-11-00103.1
- Mougin, E., P. Hiernaux, L. Kergoat, M. Grippa, P. De Rosnay, F. Timouk, and T. Lebel. 2009. The AMMA-CATCH Gourma observatory site in Mali: Relating climatic variations to changes in vegetation, surface hydrology, fluxes and natural resources. *J. Hydrol.* 375:14–33. doi:10.1016/j.jhydrol.2009.06.045
- Naabil, E., B.L. Lamptey, J. Arnault, A. Olufayo, and H. Kunstmann. 2017. Water resources management using the WRF-Hydro modelling system: Case-study of the Tono dam in West Africa. *J. Hydrol.: Reg. Studies* 12:196–209. doi:10.1016/j.ejrh.2017.05.010
- Nicholson, S. 2013. The West African Sahel: A review of recent studies on the rainfall regime and its interannual variability. *ISRN Meteorol.* 2013:453521. doi:10.1155/2013/453521
- Nicholson, S.E., C. Funk, and A.H. Fink. 2018. Rainfall over the African continent from the 19th through the 21st century. *Global Planet. Change* 165:114–127. doi:10.1016/j.gloplacha.2017.12.014
- Odekunle, T. 2004. Rainfall and the length of the growing season in Nigeria. *Int. J. Climatol.* 24:467–479. doi:10.1002/joc.1012
- Ouedraogo, I., P. Savadogo, M. Tigabu, R. Cole, P.C. Odén, and J.M. Ouadba.

2009. Is rural migration a threat to environmental sustainability in southern Burkina Faso? *Land Degrad. Dev.* 20:217–230. doi:10.1002/ldr.910
- Ouedraogo, I., P. Savadogo, M. Tigabu, S.D. Dayamba, and P.C. Odén. 2011. Systematic and random transitions of land-cover types in Burkina Faso, West Africa. *Int. J. Remote Sens.* 32:5229–5245. doi:10.1080/01431161.2010.495095
- Poméon, T., B. Diekkrüger, A. Springer, J. Kusche, and A. Eicker. 2018. Multi-objective validation of SWAT for sparsely-gauged West African river basins: A remote sensing approach. *Water* 10:451. doi:10.3390/w10040451
- Qasim, M., S. Porembski, D. Sattler, K. Stein, A. Thiombiano, and A. Lindner. 2016a. Vegetation structure and carbon stocks of two protected areas within the south-Sudanian savannas of Burkina Faso. *Environments* 3:25. doi:10.3390/environments3040025
- Qasim, M., S. Porembski, K. Stein, and A. Lindner. 2016b. Rapid assessment of key structural elements of different vegetation types of West African savannas in Burkina Faso. *J. Landscape Ecol.* 9:36–48. doi:10.1515/jlecol-2016-0003
- Qu, W., H.R. Bogena, J.A. Huisman, M. Schmidt, R. Kunkel, A. Weuthen, and H. Vereecken. 2016. The integrated water balance and soil data set of the Rollesbroich hydrological observatory. *Earth Syst. Sci. Data* 8:517–529. doi:10.5194/essd-8-517-2016
- Quansah, E., G. Katata, M. Mauder, T. Annor, L.K. Amekudzi, A.A. Balogun, et al. 2017. Assessment of simulated energy fluxes over a grassland ecosystem in the West African Sudanian Savanna. *Adv. Meteorol.* 2017:6258180. doi:10.1155/2017/6258180
- Quansah, E., M. Mauder, A.A. Balogun, L.K. Amekudzi, L. Hingerl, J. Bliefernicht, and H. Kunstmann. 2015. Carbon dioxide fluxes from contrasting ecosystems in the Sudanian Savanna in West Africa. *Carbon Balance Manage.* 10:1. doi:10.1186/s13021-014-0011-4
- Ringgaard, R., M. Herbst, T. Friberg, K. Schelde, A.G. Thomsen, and H. Soegaard. 2011. Energy fluxes above three disparate surfaces in a temperate mesoscale coastal catchment. *Vadose Zone J.* 10:54–66. doi:10.2136/vzj2009.0181
- Rosero, E., Z.L. Yang, L.E. Gulden, G.Y. Niu, and D.J. Gochis. 2009. Evaluating enhanced hydrological representations in Noah LSM over transition zones: Implications for model development. *J. Hydrometeorol.* 10:600–622. doi:10.1175/2009JHM1029.1
- Salack S., C. Klein, A. Giannini, B. Sarr, O.N. Worou, N. Belko, et al. 2016. Global warming induced hybrid rainy seasons in the Sahel. *Environ. Res. Lett.* 11:104008. doi:10.1088/1748-9326/11/10/104008
- Salack, S., I.A. Saley, and J. Bliefernicht, 2018a. Observed data of extreme rainfall events over the West African Sahel. *Data Brief* 20:1274–1278. doi:10.1016/j.dib.2018.09.001
- Salack, S., A.I. Saley, I. Zabré, Z.N. Lawson, and K.E. Daaku. 2018b: Scales for rating heavy rainfall events in the West African Sahel. *Weather Clim. Extremes* 21:36–42. doi:10.1016/j.wace.2018.05.004
- Schmid, H.P. 1997. Experimental design for flux measurements: Matching scales of observations and fluxes. *Agric. Meteorol.* 87:179–200. doi:10.1016/S0168-1923(97)00011-7
- Séguis, L., N. Boulain, B. Cappelaere, J.M. Cohard, G. Favreau, S. Galle, and D. Ramier. 2011a. Contrasted land-surface processes along the West African rainfall gradient. *Atmos. Sci. Lett.* 12:31–37. doi:10.1002/asl.327
- Séguis, L., B. Kamagaté, G. Favreau, M. Desclotres, J.L. Seidel, S. Galle, and S. van Exter. 2011b. Origins of streamflow in a crystalline basement catchment in a sub-humid Sudanian zone: The Donga basin (Benin, West Africa): Inter-annual variability of water budget. *J. Hydrol.* 402:1–13. doi:10.1016/j.jhydrol.2011.01.054
- Senatore, A., G. Mendicino, D.J. Gochis, W. Yu, D.N. Yates, and H. Kunstmann. 2015. Fully coupled atmosphere-hydrology simulations for the central Mediterranean: Impact of enhanced hydrological parameterization for short and long time scales. *J. Adv. Model. Earth Syst.* 7:1693–1715. doi:10.1002/2015MS000510
- Smith, J.W., A.E. Reynolds, A.S. Pratt, S. Salack, B. Klotz, T.L. Battle, et al. 2012. Observations of an 11 September Sahelian squall line and Saharan air layer outbreak during NAMMA-06. *Int. J. Geophys.* 2012:153256. doi:10.1155/2012/153256
- Soltani, M., M. Mauder, P. Laux, and H. Kunstmann. 2017. Turbulent flux variability and energy balance closure in the TERENO prealpine observatory: A hydrometeorological data analysis. *Theor. Appl. Climatol.* 133:937–956. doi:10.1007/s00704-017-2235-1
- Stein, K., D. Coulibaly, K. Stenchly, D. Goetze, S. Porembski, A. Lindner, S. Konaté, and K.E. Linsenmair. 2017. Bee pollination increases yield quantity and quality of cash crops in Burkina Faso, West Africa. *Sci. Rep.* 7:17691. doi:10.1038/s41598-017-17970-2
- Stisen, S., K.H. Jensen, I. Sandholt, and D.I. Grimes. 2008. A remote sensing driven distributed hydrological model of the Senegal River basin. *J. Hydrol.* 354:131–148. doi:10.1016/j.jhydrol.2008.03.006
- Tagesson, T., R. Fensholt, I. Guiro, M.O. Rasmussen, S. Huber, C. Mbow, et al. 2015. Ecosystem properties of semiarid savanna grassland in West Africa and its relationship with environmental variability. *Global Change Biol.* 21:250–264. doi:10.1111/gcb.12734
- Takagi, K., and H.S. Lin. 2011. Temporal dynamics of soil moisture spatial variability in the Shale Hills Critical Zone Observatory. *Vadose Zone J.* 10:832–842. doi:10.2136/vzj2010.0134
- Taylor, C.M., D. Belušić, F. Guichard, D.J. Parker, T. Vischel, O. Bock, and G. Panthou. 2017. Frequency of extreme Sahelian storms tripled since 1982 in satellite observations. *Nature* 544:475–478. doi:10.1038/nature22069
- Timouk, F., L. Kergoat, E. Mougou, C. Lloyd, E. Ceschia, P. De Rosnay, et al. 2009. Response of surface energy balance to water regime and vegetation development in a Sahelian landscape. *J. Hydrol.* 375:178–189. doi:10.1016/j.jhydrol.2009.04.022
- Van De Giesen, N., H. Kunstmann, G. Jung, J. Liebe, M. Andreini, and P.L. Vlek. 2002. The GLOWA Volta project: Integrated assessment of feedback mechanisms between climate, landuse, and hydrology. In: M. Beniston, editor, *Climatic change: Implications for the hydrological cycle and for water management* Springer, Dordrecht, the Netherlands. p. 151–170. doi:10.1007/0-306-47983-4\_9
- van Roosmalen, L., T.O. Sonnenborg, K.H. Jensen, and J.H. Christensen. 2011. Comparison of hydrological simulations of climate change using perturbation of observations and distribution-based scaling. *Vadose Zone J.* 10:136–150. doi:10.2136/vzj2010.0112
- Vischel, T., T. Lebel, S. Massuel, and B. Cappelaere. 2009. Conditional simulation schemes of rain fields and their application to rain-fall-runoff modeling studies in the Sahel. *J. Hydrol.* 375:273–286. doi:10.1016/j.jhydrol.2009.02.028
- Verhoef, A., S.J. Allen, H.A.R. De Bruin, C.M.J. Jacobs, and B.G. Heusinkveld. 1996. Fluxes of carbon dioxide and water vapour from a Sahelian savanna. *Agric. For. Meteorol.* 80:231–248. doi:10.1016/0168-1923(95)02294-5
- Wallace, J.S., I.R. Wright, J.B. Stewart, and C.J. Holwill. 1991. The Sahelian Energy Balance Experiment (SEBEX): Ground based measurements and their potential for spatial extrapolation using satellite data. *Adv. Space Res.* 11:131–141. doi:10.1016/0273-1177(91)90413-E
- White, F. 1983. *The vegetation of Africa*. United Nations Educ. Sci. Cultural Org., Paris.
- Wollschläger, U., S. Attinger, D. Borchardt, M. Brauns, M. Cuntz, P. Dietrich, and A. Hildebrandt. 2017. The Bode hydrological observatory: A platform for integrated, interdisciplinary hydro-ecological research within the TERENO Harz/Central German Lowland Observatory. *Environ. Earth Sci.* 76:29. doi:10.1007/s12665-016-6327-5
- Yira, Y., B. Diekkrüger, G. Steup, and A.Y. Bossa. 2016. Modeling land use change impacts on water resources in a tropical West African catchment (Dano, Burkina Faso). *J. Hydrol.* 537:187–199. doi:10.1016/j.jhydrol.2016.03.052
- Yucel, I., A. Onen, K.K. Yilmaz, and D.J. Gochis. 2015. Calibration and evaluation of a flood forecasting system: Utility of numerical weather prediction model, data assimilation and satellite-based rainfall. *J. Hydrol.* 523:49–66. doi:10.1016/j.jhydrol.2015.01.042
- Zacharias, S., H. Bogena, L. Samaniego, M. Mauder, R. Fuß, T. Pütz, et al. 2011. A network of terrestrial environmental observatories in Germany. *Vadose Zone J.* 10:955–973. doi:10.2136/vzj2010.0139